REPORT No. 184 S
(S 3/167, 280, S 90/178, 180, 229, 229a)

December 1973

NEDERLANDS SCHEEPSSTUDIECENTRUM TNO
NETHERLANDS SHIP RESEARCH CENTRE TNO
SHIPBUILDING DEPARTMENT LEEGHWATERSTRAAT 5, DELFT

★

NUMERICAL AND EXPERIMENTAL VIBRATION ANALYSIS OF A DECKHOUSE

(NUMERIEK EN EXPERIMENTEEL TRILLINGSONDERZOEK AAN EEN DEKHUIS)

by

DR. IR. P. MEIJERS
IR. W. TEN CATE
IR. L. J. WEVERS
(Institute TNO for Mechanical Constructions)

IR. J. H. VINK
(Netherlands Ship Research Centre TNO)

Issued by the Council

VOORWOORD

Met behulp van de eindige elementenmethode is het mogelijk geworden op eenvoudige wijze de stijfheidsverdeling van gecompliceerde constructies, zoals een dekhuis, te bepalen. Daarna kunnen dan met standaard computerprogramma's trillingsrekeningen voor dergelijke constructies worden uitgevoerd.

Voor een scheepsontwerp is het van belang reeds in een vroeg stadium de eigenfrequenties van de bovenbouw te kennen teneinde nog in staat te zijn de excitatie-frequenties van de schroef of de stijfheidsverdeling van het dekhuis aan te passen ter voorkoming van trillingshinder. Het is om deze reden wenselijk dat wordt nagegaan of voldoende nauwkeurigheid kan worden bereikt met de nog zeer globale ontwerpgegevens betreffende massaverdeling en geometrie.

Bij constructies, die zo ongelijkmatig zijn opgebouwd als een dekhuis, moet een zekere schematisering worden toegepast. Verder wordt in verband met de omvang van de berekening bij voorkeur een lokale berekening uitgevoerd, waarbij de koppeling met de rest van het schip verwaarloosd wordt. Teneinde het effect van deze vereenvoudiging te kunnen vaststellen, is het ook zinvol de berekende resultaten experimenteel te verifiëren.

Een dergelijk theoretisch onderzoek, geverifieerd door experimenten, kon worden uitgevoerd voor het brugdekhuis van de „TRIDENT" schepen van de Koninklijke Nederlandse Stoomboot Maatschappij en is mede tot stand gekomen door industriële bijdragen van de Koninklijke Nederlandse Redersvereniging.

HET NEDERLANDS SCHEEPSSTUDIECENTRUM TNO

PREFACE

With help of the finite element method it has become possible to determine in a simple way the stiffness distribution of complicated structures as a deckhouse. Afterwards the dynamic behaviour of such structures may be analyzed with standard computer programs.

For a ship it is important to know the natural frequencies of the superstructure in an early design stage, in order to be able to adapt the excitation frequencies of the screw or the stiffness distribution of the deckhouse to prevent vibration troubles. It is for this reason desirable to investigate whether or not a sufficient accuracy can be obtained with the still very global design specifications with respect to mass distribution and geometry.

For such a complicated structure as a deckhouse a certain modelling has always to be performed. Moreover, it is preferable because of the extension of the calculations to carry out a local analysis and to neglect the coupling with the rest of the ship. In order to determine the effects of such simplifications it is also useful to verify the numerical results with experiments.

Such a theoretical analysis verified with experiments could be carried out for the bridge deckhouse of the "TRIDENT" ships of the Koninklijke Nederlandse Stoomboot Maatschappij and it has partly been achieved by the industrial support of the Koninklijke Nederlandse Redersvereniging.

THE NETHERLANDS SHIP RESEARCH CENTRE TNO

CONTENTS

LIST OF SYMBOLS

A	Cross sectional area
A^p	Area where pressure is prescribed
A_{pl}	Area cross-section plate element
A_{xs}	Area cross-section stiffener in x-direction
A_{ys}	Area cross-section stiffener in y-direction
E	Young's modulus
E_1, E_2	Young's moduli orthotropic plate
E_c	Complementary energy
G	Shear modulus
G_{12}	Shear modulus orthotropic plate
H	Functional
I_x, I_y, I_z	Moments of inertia
K	Stiffness matrix
K^*	Condensed stiffness matrix
M	Mass matrix
M^*	Condensed mass matrix
R	Radius
T	Transformation matrix
V	Volume
a^k	Vector of displacement parameters
d_k	Thickness plate element k
l	Length of bar element
m	Mass
p_i	Components of pressure vector
u	Structural displacement vector
u_i	Displacement components
$\bar{u}^k$	Element displacement vector in local coordinate system
u^k	Element displacement vector in global coordinate system
$\tilde{u}$	Displacement function for displacement in x-direction
v	Structural displacement vector
$\tilde{v}$	Displacement function for displacements in y-direction
$\tilde{w}$	Displacement function for displacements in z-direction
x_i	Coordinates
$\bar{x}$	Local coordinate
$\bar{y}$	Local coordinate
$\varepsilon_x, \varepsilon_y$	Normal strain components
γ_{xy}	Shear strain component
ν	Poisson's ratio
ν_{12}, ν_{21}	Poisson's ratios orthotropic plate
ϱ	Specific mass
σ_{ij}	Stress tensor
$\sigma_x, \sigma_y, \sigma_z$	Normal stress components
σ^k	Vector of stress parameters
σ_{xp}, σ_{yp}	Normal stresses in plate
ω	Circular frequency

NUMERICAL AND EXPERIMENTAL VIBRATION ANALYSIS OF A DECKHOUSE

by

Dr. Ir. P. MEIJERS, Ir. W. TEN CATE, Ir. L. J. WEVERS and Ir. J. H. VINK

Summary

With a finite element analysis the lower natural frequencies and the corresponding vibration modes of a deckhouse have been determined with accurate data and again with data for the mass distribution and geometry as available in an early design stage. To check the approximations introduced in the analysis an experiment was carried out for verification. The experimental and theoretical results turn out to be in good agreement.

1 Introduction

The last few years repeatedly serious vibrational inconvenience was experienced in deckhouses of ships. In order to prevent such an inconvenience for ships to be built, one should be able to predict the dynamic behaviour as early as possible in the design stage.

Theoretical vibration analysis for structures as complicated as deckhouses can only accurately be performed with numerical methods. And even when these numerical methods are applied to determine the stiffness distribution of a superstructure, which is often built up very irregularly, a simplification in the description of the geometry is advisable to restrict the computation cost. Such a modelling, however, introduces errors for which it is fairly difficult to give a reliable estimate.

Another simplification in the numerical calculations to be presented in this report is the assumption that the rest of the ship is so stiff with respect to the deckhouse, that a good approximation for the lower natural frequencies of the deckhouse can be obtained assuming it rigidly clamped in the maindeck.

The analysis has been carried out not only for the real structure with an accurately determined mass distribution but also with information available during the early design stage when only the global geometry is fixed and a guess of the total mass and the mass distribution has to be made with help of previously built deckhouses. It was hoped that even with such a coarse approximation it would be possible to arrive at a fairly accurate estimate of the lower natural frequencies, since these lower frequencies are not very sensitive for local deviations of an assumed mass- and stiffness distribution.

To determine the total effect of the simplifications

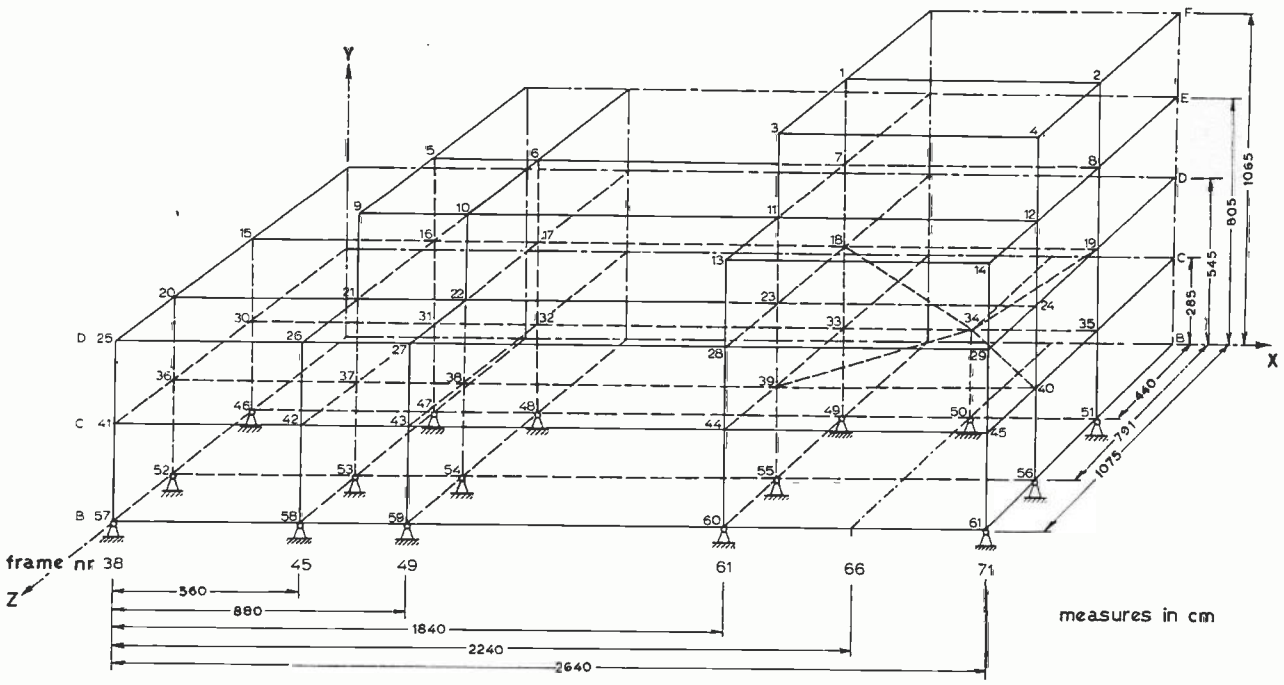

Fig. 1. Modelled deckhouse.

in the theoretical analysis, the lower natural frequencies and the vibration modes have also been measured.

The construction of the deckhouse is according to the inserted drawing: KNSM-Ships. Construction Plan Bridge Deckhouse. Building No. 664/665. Drawing No. 16 of Engineering Works and Shipyard P. Smit Jr. N.V. Rotterdam, Shipbuilding Department.

2 Finite element analysis

2.1 *Modelling of the structure*

The chosen grid of nodal points for the finite element analysis is according to fig. 1. Apart from small details the structure is symmetric with respect to the x-y-plane and therefore the whole structure can be analyzed by determining separately the vibration modes that are symmetric and antisymmetric with respect to the plane x-y for the indicated half of the structure.

The element types chosen are bar elements, rectangular and triangular orthotropic membrane elements. All these elements are for this structure parallel to the coordinate planes. Most of the plate fields are stiffened in one direction and some in two directions, see fig. 2. Such a plate field is replaced by a fictitious orthotropic plate element with thickness equal to the thickness of the original plate while the influence of the stiffeners is accounted for by adjusting the elastic constants of the element, see Appendix I.

In many cases the longitudinal and transverse bulkheads are not placed in line on the different levels of the deckhouse as will be clear from the construction drawing, and in this report the effect of these irregularities on the stiffness distribution is also incorporated in the elastic constants of the plate elements. The effect of holes and local stiffening are of course also taken into account in the effective elastic constants of the corresponding element. The stiffness of intermediate bulkheads is added as accurately as possible to the stiffness of the nearest membrane elements of the model structure.

In several cases the element boundaries of the model structure do not fit with the boundaries in the real structure. In these cases the stiffness and mass distribution are adapted in such a way that one can expect the lower natural frequencies of the model plate with connected mass to be approximately the same as for the corresponding plate in the real structure.

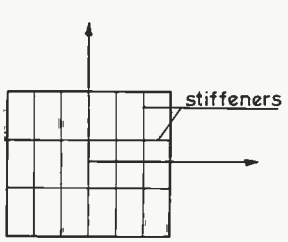

Fig. 2. Stiffened platefield.

The required information for the determination of the mass distribution is taken from [1] and for the steelstructure from the construction plan. In general the mass is spread statically over the surrounding nodal points.

The centre of gravity of furniture, walls and plumbing is taken at 500 mm above the floor and uniformly distributed over the area of the deck. The mass of piping, ventilation shafts, electrical cables and switch boards is taken uniformly distributed over the wall surfaces. The mass of staircases, steps, etc. in the casing of the engine room is assumed uniformly distributed over the volume of the casing. A number of heavy members were handled in a special way as discussed in Appendix II.

To determine the lower natural frequencies of a structure it is in general possible to solve an eigenvalue problem with far fewer degrees of freedom than are required to determine accurately the stiffness distribution of the structure. Therefore, having obtained the mass and stiffness distribution a condensation to a smaller number of freedoms will be carried out. The choice which of the freedoms are "master" freedoms and which are "slaves" is also an important part of the modelling and requires insight in the dynamic behaviour of structures.

2.2 *Element stiffness matrices*

First the rectangular orthotropic membrane elements are considered, see fig. 3. To obtain an approximate solution for the stiffness matrix of such an element, the variational principle of Reissner will be applied. This principle states that in case of an exact solution the expression:

$$H = \iiint_V \left[\tfrac{1}{2}\sigma_{ij}\left(\frac{\partial u_i}{\partial x_j} + \frac{\partial u_j}{\partial x_i}\right) - E_c \right] \mathrm{d}V - \iiint_V \varrho f_i u_i \,\mathrm{d}V - \iint_{A_p} p_i u_i \,\mathrm{d}A \qquad (1)$$

is stationary with respect to all kinematically allowable variations of the components of the displacement-vector u_i and with respect to all variations of the components of the stress tensor σ_{ij}.

Assuming an approximate displacement field with a number of displacement parameters and at the same time an approximate stress distribution with a set of stress parameters, one can expect to obtain an approximate solution by stating that H must be stationary with respect to all stress and displacement parameters.

Fig. 3 shows an aribtrary membrane element k in a local coordinate system $\bar{x}$-$\bar{y}$. When the material behaves

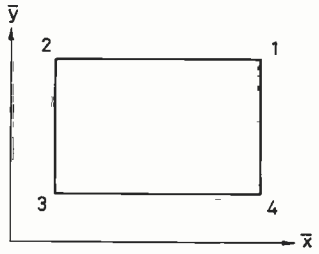

Fig. 3. Rectangular membrane element

linearly elastic the following stress-strain relations hold for the state of plane stress in an orthotropic plate:

$$\begin{vmatrix} \varepsilon_x \\ \varepsilon_y \\ \gamma_{xy} \end{vmatrix} = \begin{vmatrix} c_{11} & c_{12} & 0 \\ c_{21} & c_{22} & 0 \\ 0 & 0 & c_{33} \end{vmatrix} \begin{vmatrix} \sigma_x \\ \sigma_y \\ \tau_{xy} \end{vmatrix} \tag{2}$$

where:

$$c_{11} = \frac{1}{E_1},$$

$$c_{12} = -\frac{\nu_{21}}{E_2},$$

$$c_{21} = -\frac{\nu_{12}}{E_1},$$

$$c_{22} = \frac{1}{E_2},$$

$$c_{33} = \frac{1}{G_{12}},$$

and the complementary energy per unit volume is for such a linear-elastic plate:

$$E_c = \tfrac{1}{2}|\sigma_x \sigma_y \tau_{xy}| \begin{vmatrix} c_{11} & c_{12} & 0 \\ c_{21} & c_{22} & 0 \\ 0 & 0 & c_{33} \end{vmatrix} \begin{vmatrix} \sigma_x \\ \sigma_y \\ \tau_{xy} \end{vmatrix} \tag{3}$$

The approximate displacement functions over an element are chosen to be the following polynomials:

$$\begin{aligned} \tilde{u} &= a_1 + a_2\bar{x} + a_3\bar{y} + a_4\bar{x}\bar{y} \\ \tilde{v} &= a_5 + a_6\bar{x} + a_7\bar{y} + a_8\bar{x}\bar{y} \\ \tilde{w} &= 0 \end{aligned} \tag{4}$$

and the assumed stress distribution is:

$$\begin{aligned} \sigma_x &= \sigma_1 + \sigma_2\bar{y} \\ \sigma_y &= \sigma_3 + \sigma_4\bar{x} \\ \tau_{xy} &= \sigma_5 \\ \sigma_z &= \tau_{yz} = \tau_{zx} = \end{aligned} \tag{5}$$

The displacement- and stress-distribution are equal to the distributions assumed by Visser [2] for an isotropic plate-element. The assumed constant shear stress is more realistic than the approximate shear-stress-distribution obtained by assuming for $\tilde{u}$ and $\tilde{v}$ the displacement field indicated in (4) and minimizing the potential energy with respect to the displacement parameters.

The vector of displacement parameters a_i for element k are collected in the vector a^k and the stress parameters σ_i in vector σ^k. Substitution of (4) and (5) into (1) yields for an isolated element the discrete analogue of (1)

$$H = -\tfrac{1}{2}\sigma'^k F^k \sigma^k + \sigma'^k W^k a^k - f'^k a^k \tag{6}$$

where for the plate element:

$$F^k = \begin{vmatrix} c_{11}\chi_0^0 & & & & \text{(symmetric)} \\ c_{11}\chi_1^0 & c_{11}\chi_2^0 & & & \\ c_{21}\chi_0^0 & c_{21}\chi_1^0 & c_{22}\chi_0^0 & & \\ c_{21}\chi_0^1 & c_{21}\chi_1^1 & c_{22}\chi_0^1 & c_{22}\chi_0^2 & \\ 0 & 0 & 0 & 0 & \chi_0^0 \end{vmatrix} \tag{7}$$

and

$$W^k = \begin{vmatrix} 0 & \chi_0^0 & 0 & \chi_1^0 & 0 & 0 & 0 & 0 \\ 0 & \chi_1^0 & 0 & \chi_2^0 & 0 & 0 & 0 & 0 \\ 0 & 0 & 0 & 0 & 0 & 0 & \chi_0^0 & \chi_0^1 \\ 0 & 0 & 0 & 0 & 0 & 0 & \chi_0^1 & \chi_0^2 \\ 0 & 0 & \chi_0^0 & \chi_0^1 & 0 & \chi_0^0 & 0 & \chi_1^0 \end{vmatrix} \tag{8}$$

The volume integrals χ_q^p are defined to be:

$$\chi_q^p = \mathrm{d}_k \iint_{A^k} \bar{x}^p \bar{y}^q \,\mathrm{d}\bar{x}\,\mathrm{d}\bar{y} \tag{9}$$

Vector f^k is a loading vector.

The expression for H is stationary with respect to variations of the stress parameters when:

$$\sigma^k = [F^k]^{-1} W^k a^k \tag{10}$$

Substitution of (10) into (6) provides the following expression for the complementary elastic energy in terms of the displacement parameters a^k:

$$E_c^k = \tfrac{1}{2}a'^k W'^k [F^k]^{-1} W^k a^k = \tfrac{1}{2}a'^k S^k a^k \tag{11}$$

This complementary energy is for linear elastic problems equal to the strain energy and hence S^k can be considered as a modified stiffness matrix. Here the term modified stiffness matrix is used to distinguish between the stiffness matrix that would have been obtained when the stress parameters had not been chosen as degrees of freedom, but the stresses had been

derived directly applying Hooke's law to the derivatives of the chosen displacement functions.

When the vector of displacement-freedoms of the corner points in the local coordinate system is defined to be:

$$\bar{u}'^k = |\bar{u}_1\bar{v}_1\bar{u}_2\bar{v}_2\bar{u}_3\bar{v}_3\bar{u}_4\bar{v}_4| \tag{12}$$

the strain energy may also be written in the form:

$$E_u^k = \tfrac{1}{2}\bar{u}'^k D'^k S^k D^k \bar{u}^k \tag{13}$$

where the inverse of the matrix D^k relating the displacement-parameters to the nodal point displacements is:

$$[D^k]^{-1} = \begin{vmatrix} 1 & \bar{x}_1 & \bar{y}_1 & \bar{x}_1\bar{y}_1 & 0 & 0 & 0 & 0 \\ 0 & 0 & 0 & 0 & 1 & \bar{x}_1 & \bar{y}_1 & \bar{x}_1\bar{y}_1 \\ 1 & \bar{x}_2 & \bar{y}_2 & \bar{x}_2\bar{y}_2 & 0 & 0 & 0 & 0 \\ 0 & 0 & 0 & 0 & 1 & \bar{x}_2 & \bar{y}_2 & \bar{x}_2\bar{y}_2 \\ 1 & \bar{x}_3 & \bar{y}_3 & \bar{x}_3\bar{y}_3 & 0 & 0 & 0 & 0 \\ 0 & 0 & 0 & 0 & 1 & \bar{x}_3 & \bar{y}_3 & \bar{x}_3\bar{y}_3 \\ 1 & \bar{x}_4 & \bar{y}_4 & \bar{x}_4\bar{y}_4 & 0 & 0 & 0 & 0 \\ 0 & 0 & 0 & 0 & 1 & \bar{x}_4 & \bar{y}_4 & \bar{x}_4\bar{y}_4 \end{vmatrix} \tag{14}$$

With a transformation matrix T^k the displacement vector in the local coordinate system is related to the element displacement-vector in the global system:

$$u'^k = |u_1v_1w_1u_2v_2w_2u_3v_3w_3u_4v_4w_4| \tag{15}$$

and a so-called location matrix L^k relates the element displacement-vector u^k to the structural vector u. The contribution of an arbitrary element k to the structural strain energy is in terms of the global displacement-vector:

$$E_u^k = \tfrac{1}{2}u' K^k u \tag{16}$$

where:

$$K^k = L^k T'^k D'^k S^k D^k T^k L^k \tag{17}$$

Besides the rectangular membrane elements a few orthotropic triangular membrane elements with 3 nodal points (TRIM-3) have been applied, see fig. 4. These elements are constant stress elements, the displacement functions are in the local coordinate system:

$$\begin{aligned} \tilde{u} &= a_1 + a_2\bar{x} + a_3\bar{y} \\ \tilde{v} &= a_4 + a_5\bar{x} + a_6\bar{y} \end{aligned} \tag{18}$$

The TRIM-3 elements are somewhat less accurate than the applied rectangular elements and therefore they are used only when pressed by the geometry of the structure. Application of Reissner's principle on element scale is not useful because the result would be exactly the same as when the more straight forward method of minimum potential energy is applied.

In terms of the vector of displacement parameters a^k the elastic energy for an arbitrary element k is:

$$E_u^k = \tfrac{1}{2}a'^k S^k a^k \tag{19}$$

where for this element type:

$$S^k = V^k \begin{vmatrix} 0 & & & & & \text{(symmetric)} \\ 0 & s_{22} & & & & \\ 0 & 0 & s_{33} & & & \\ 0 & 0 & 0 & 0 & & \\ 0 & 0 & s_{53} & 0 & s_{55} & \\ 0 & s_{62} & 0 & 0 & 0 & s_{66} \end{vmatrix} \tag{20}$$

and

$$s_{22} = \frac{E_1}{(1-\nu_{12}\nu_{21})}; s_{33} = s_{53} = s_{55} = G_{12};$$

$$s_{62} = \frac{\nu_{12}E_2}{(1-\nu_{12}\nu_{21})}; s_{66} = \frac{E_2}{(1-\nu_{12}\nu_{21})}$$

The element displacement-vector in the local coordinate system is for the triangular element:

$$\bar{u}'^k = |\bar{u}_1\bar{v}_1\bar{u}_2\bar{v}_2\bar{u}_3\bar{v}_3| \tag{21}$$

and the matrix relating a^k to $\bar{u}^k$ is in terms of the nodal point coordinates:

$$[D^k]^{-1} = \begin{vmatrix} 1 & \bar{x}_1 & \bar{y}_1 & 0 & 0 & 0 \\ 0 & 0 & 0 & 1 & \bar{x}_1 & \bar{y}_1 \\ 1 & \bar{x}_2 & \bar{y}_2 & 0 & 0 & 0 \\ 0 & 0 & 0 & 1 & \bar{x}_2 & \bar{y}_2 \\ 1 & \bar{x}_3 & \bar{y}_3 & 0 & 0 & 0 \\ 0 & 0 & 0 & 1 & \bar{x}_3 & \bar{y}_3 \end{vmatrix} \tag{22}$$

The elements are again parallel to one of the coordinate planes and hence with a simple transformation matrix and a location matrix one can obtain the contribution of an arbitrary element to the global stiffness matrix. The formal expression becomes again as indicated in (16).

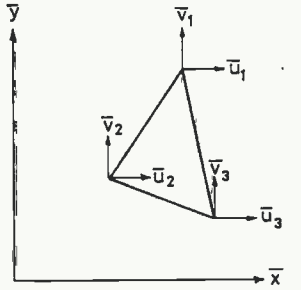

Fig. 4. Triangular membrane element

Apart from the stiffeners on the plate elements that are incorporated in the stiffness of the plates, a number of stiffeners along the boundaries of the elements is treated separately. All these elements are parallel to one of the coordinate axes. The axial displacements are assumed to vary linearly along the stiffeners and the degrees of freedom are the displacements at the end of the stiffeners. These are the simplest possible stiffener elements and they are compatible with the displacements of the neighbouring plate elements.

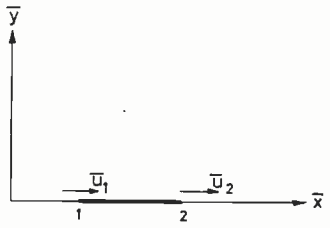

Fig. 5. Stiffener element

The displacement-vector in the local coordinate system is:

$$\bar{u}'^{k} = |\bar{u}_1 \bar{u}_2| \tag{23}$$

and the contribution to the strain energy may again be written formally as indicated in (16) where for the stiffener element:

$$K^k = \begin{vmatrix} \frac{EA_s}{l} & -\frac{EA_s}{l} \\ -\frac{EA_s}{l} & \frac{EA_s}{l} \end{vmatrix} \tag{24}$$

2.3 *Eigenvalue analysis*

Superposition of all the contributions of the individual elements discussed in paragraph 2.2 yields the strain energy of the whole structure:

$$E_u = \tfrac{1}{2} u' K u \tag{25}$$

The mass matrix is in the discrete description defined such that the vector of inertia forces is:

$$-M\ddot{u} \tag{26}$$

Most of the mass distribution of the deckhouse is discretized directly as point masses at the nodal points. These point masses only contribute to the diagonal terms of the mass matrix. However, a number of heavy parts are handled separately as discussed in Appendix II and they give also contribution to the non-diagonal terms. A more detailed information with respect to the stiffness and mass distribution is given in [3].

Apart from the inertia forces there will in general be a time-dependent external loading on the system. This external loading can consistently be reduced to a vector $f(t)$ of forces coupled with the chosen degrees of freedom.

The damping forces are neglected since it is not possible to give a reliable estimate of the damping matrix and moreover the damping will hardly influence the natural frequences to be determined.

For an arbitrary but kinematically allowable variation of the displacement vector (δu), the variation of the elastic energy is equal to the virtual work of the inertia forces and the external forces. This yields the set of second order differential equations for the components of the displacement vector:

$$M\ddot{u} + Ku = f(t) \tag{27}$$

By classical means one can obtain the natural frequencies and the response of the dynamic system described by (27). Only the determination of the natural frequencies will be discussed here.

When the number of degrees of freedom is large the determination of the natural frequencies is rather computertime-consuming. Moreover, it is known that for calculating a set of lower natural frequencies the system can have far fewer degrees of freedom than is required to determine the stiffness matrix with sufficient accuracy. Therefore a condensation to a smaller system will be carried out. The procedure to be followed has been indicated by Irons et al. [4].

The displacement-vector is split up as follows:

$$u' = |u_1' u_2'| \tag{28}$$

where u_1 indicates the degrees of freedom that are in the condensed system coupled with mass ("master freedoms") and vector u_2 collects the remaining freedoms ("slaves"). The same splitting is carried out for the stiffness and mass matrix:

$$K = \begin{vmatrix} K_{11} & K_{12} \\ K_{21} & K_{22} \end{vmatrix}, \quad M = \begin{vmatrix} M_{11} & M_{12} \\ M_{21} & M_{22} \end{vmatrix} \tag{29}$$

The stiffness matrix for the condensed system, which indicates the relation between the master-freedoms and the forces coupled with these freedoms is:

$$K^* = K_{11} - K_{12} K_{22}^{-1} K_{21} \tag{30}$$

and the displacement-vector u_2 is in terms of u_1:

$$u_2 = -K_{22}^{-1} K_{21} u_1 \tag{31}$$

The virtual work of the inertia forces for kinematically admissible variations of vector u is:

$$\delta u' M u \tag{32}$$

and when from this equation u_2 is eliminated one obtains:

$$\delta u_1' M^* u_1 \tag{33}$$

where:

$$M^* = M_{11} - M_{12}K_{22}^{-1}K_{21} - K_{12}K_{22}^{-1}M_{21} + \\ + K_{12}K_{22}^{-1}M_{22}K_{22}^{-1}K_{21} \tag{34}$$

In case M is a diagonal matrix expression (34) simplifies considerably but even then M^* is not a diagonal matrix.

Now the natural frequencies of the system:

$$M^*\ddot{u}_1 + K^* u_1 = 0 \tag{35}$$

are to be determined. Substitution of a displacement-vector:

$$u_1 = u_0 e^{i\omega t} \tag{36}$$

leads to the eigenvalue problem:

$$[K^* - \omega^2 M^*]u_0 = 0 \tag{37}$$

The mass matrix is decomposed according to Choleski [5] into:

$$M^* = R'R \tag{38}$$

where R is an upper-triangular matrix. With the substitution:

$$u_0 = R^{-1}r \tag{39}$$

(37) transforms into the classical form:

$$[A - \omega^2 I]r = 0 \tag{40}$$

where the symmetric positive definite matrix:

$$A = R'^{-1}K^*R^{-1} \tag{41}$$

For the solution of the eigenvalue problem (40) efficient computer-programmes are directly available.

The eigenvectors r_i are mostly normed in such a way that:

$$r_i' r_i = 1 \tag{42}$$

In that case the eigenvectors u_{0i} satisfy the relations:

$$u_{0i}' M^* u_{0j} = 1 \quad \text{for} \quad i = j \\ = 0 \quad \text{for} \quad i \neq j \tag{43}$$

It will be clear that insight in the physical nature of the problem is required in choosing the master degrees of freedom. It must be possible to describe the important vibration modes accurately with the components of u_1.

An alternative method of condensation would be that the masses are directly discretized as point masses coupled with the master degrees of freedom. The example discussed in [6] shows, however, that it is to be expected that such a discretization gives less accurate results.

3 Experiments

3.1 *Execution of the experiments*

Only the frequencies of the deckhouse that are in a frequency range for which considerable exciting forces due to the screw and the engine are to be expected, are of importance and this implies that a restriction to the lower natural frequencies can be made. The frequency range for the excitation was chosen to be 15 to 42 Hz. From the theoretical results one can expect to find the three lower symmetric and antisymmetric frequencies in this range and this is for all purposes sufficient.

The excitation of the superstructure was performed by an unbalance exciter, see fig. 6. Two indentical gears rotating in opposite direction each with an unbalanced mass furnish centrifugal forces. The vertical components of the centrifugal forces act in opposite direction and the resultant horizontal force is:

$$f = 2m\omega^2 R\cos\omega t \tag{44}$$

During the experiments the exciter was adjusted to a force amplitude [7]:

$$f = 0.055\omega^2 (N) \tag{45}$$

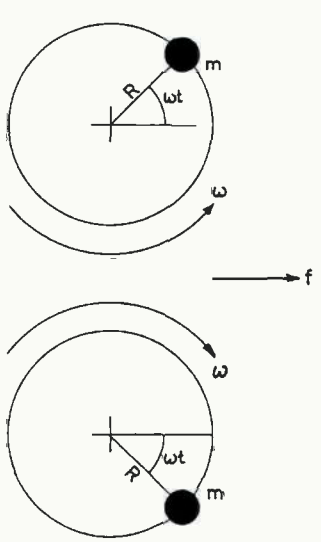

Fig. 6. Schema of unbalance exciter

where ω is the radial frequency in radials per second. The exciter was located on the *E*-deck of the ship. This deck has locally been stiffened on top and bottom-side to obtain a better load diffusion from the exciter-frame to the deckhouse.

Two series of measurements were carried out viz. with excitation in longitudinal and in transverse direction respectively. At all the nodal points in fig. 1 the accelerations in three directions were measured by Statham accelerometers. The signals were amplified by Hottinger amplifiers and subsequently recorded on magnetic tape by an Ampex registration recorder. Synchronous to the acceleration signals a so-called pulse-train was registered on the tape. The frequency of the pulses is proportional to the angular frequency of the exciter. The pulse-train was required for the analysis of the signals to be discussed in paragraph 3.2. The blockdiagram of the measuring system and of the analysis system is shown in fig. 7.

3.2 *Analysis of the experimental results*

The acceleration signals registered on magnetic tape were integrated twice and after amplification subsequently fed into a band-pass filter with constant 2 Hz band-width. Since the registered signals were played back with a speed four times faster than the recording speed the effective band-width became 0.5 Hz. The filter centre frequency was controlled by a sine wave signal originating from the pulse-train with a frequency four times the excitation frequency.

The result is that only the portion of the recorded signal with a frequency equal to that of the exciter passes the filter and the disturbances that are always present, although there is a harmonic excitation, are filtered out. The displacement amplitude as a function of the excitation frequency obtained from the registered signals were plotted on an *x*-*y*-plotter.

For some locations mobility characteristics have been computed from the displacement-frequency characteristics already mentioned. In a mobility diagram the quotient of velocity amplitude and excitation force amplitude is plotted as a function of frequency, figs. 12–17. In general these mobility plots are more suited for the determination of resonance peaks than the displacement-frequency curves discussed above. This is mainly due to the fact that a better scaling is obtained when dividing the velocity amplitudes by the force amplitude.

The phase angles of the motion of the points were determined with respect to the phase of the motion of location 34 in order to obtain the mode shapes. The *x*-axis of the oscilloscope was fed by a signal of location 34 and the vertical axis by another displacement-

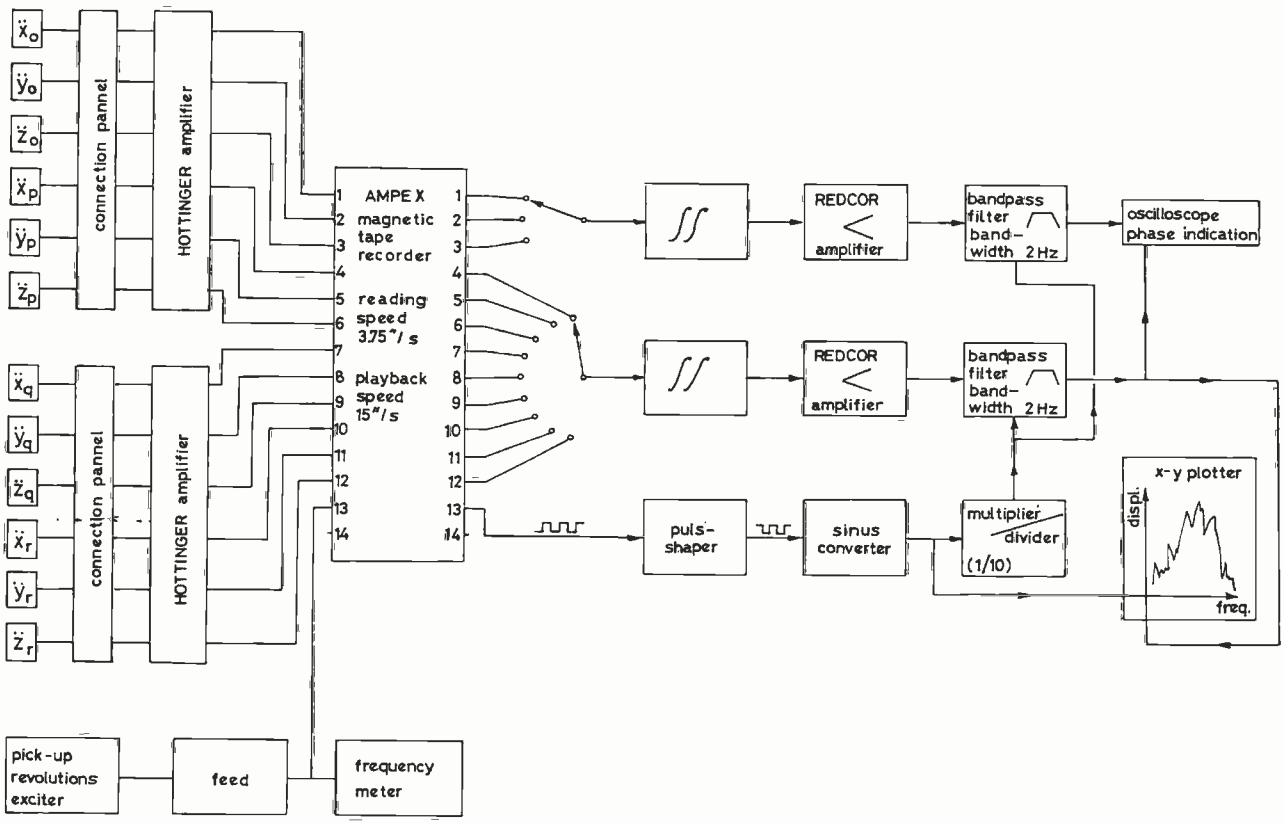

Fig. 7. Blockdiagram of measuring and analysing system.

signal. The position of the LISSAJOUS-figure obtained in this way, is an indication that the signals are either in phase or in counter-phase. More detailed information about the measurements is given in [8].

4 Calculations based upon design stage data

4.1 *Stiffness distribution*

As mentioned before the lower natural frequencies have also been calculated for an early design stage. The differences between the more accurate analysis and the approximate method to be discussed is the way of preparing the input data for the mass and stiffness distribution. It has been assumed that the overall dimensions of the deckhouse and the placing of the partition bulkheads in it are fixed.

In making an approximate construction plan of the deckhouse Lloyds Rules were used to determine plate thicknesses and scantlings of beams, frames, stiffeners, girders and pillars. In this plan the location of girders was chosen independently of the existing construction plan.

It turned out that the required plate thicknesses were all less than 7 mm, and it is common practice to increase such thin plates by some 1–1.5 mm. However, this departure from the rule thickness may be fairly important for the stiffness distribution. For that reason this point has been checked, and it was found out from the construction plan that the rule thicknesses had been increased by 1.5 mm as an average. Consequently, 1.5 mm increased thicknesses were used in this calculation for all plates too. The contributions of the elements to the stiffness matrix was calculated according to section 2.2.

4.2 *Mass distribution*

Assuming a certain mass distribution one may expect the lower frequencies to be inversely proportional to the square root of the total mass of the deckhouse and hence although the frequencies are not very sensitive for slight variations it is important to know this total mass fairly accurately.

The design forms for the total weight of deckhouses show a considerable scatter [9, 10]. Looking upon the overall dimensions of the deckhouse, a good approximation should be:

0.075 t/m^3 for steel,
0.040 t/m^3 for wood and outfit,
0.115 t/m^3 for total weight.

This results in a deckhouse weight excluding heavy apparatus of 528.0 t.

To arrive at an approximate distribution of the total mass the following procedure was used. For each layer of the deckhouse the total mass of steel, and wood plus outfit was assumed to be proportional to the volume. Then, in each layer of the deckhouse a subdivision was made to obtain a realistic mass distribution over the height. The weight of the walls was thought to be uniformly distributed. Of furniture and small apparatus 30% was concentrated in the topdeck and 70% in the bottomdeck of the layer. Finally the total weights concentrated in the decks were assumed uniformly distributed over the area of the decks. The mass of the large members and the moments of inertia were guessed. The total mass of these members was found to be 55000 kg with respect to 47278 kg in reality. The contribution of these members to the mass matrix were determined as indicated in Appendix II. The total mass of the deckhouse coupled with the chosen degrees of freedom turned out to be 566.8 t, while in reality the mass was 531.7 t.

5 Numerical results and discussion

Both for the symmetric and the antisymmetric vibrations the stiffness and mass matrix have been determined for a system with 134 degrees of freedom, and it is condensed to a system with 78 degrees of freedom for which all the natural frequencies and vibration modes have been determined. Only 5 of the lower frequencies of the symmetric and the antisymmetric vibrations are indicated in Table I, the corresponding theoretically obtained vibration modes for the two lower frequencies are indicated in figs. 8–11.

One must be aware of the fact that the vibration modes must be described with sufficient accuracy with the displacement functions chosen between the nodal points and therefore only a restricted number of the 78 frequencies can be accurate, assuming for the time being that the modelling of the real structure to the simplified box structure does not introduce any inaccuracy. But this is not of practical importance here since one is interested only in the lower frequencies.

A number of 78 master degrees of freedom was chosen because the eigenvalue analysis for such a system can be carried out for a price that is negligible with respect to the total preparation cost of such a deckhouse analysis, but it would also be possible to obtain with sufficient accuracy the 5 lower frequencies with a considerably smaller number of suitably chosen master freedoms.

Experimentally obtained mobility curves for three points during symmetric and antisymmetric excitation are shown in figs. 12–17. From these curves three natural frequencies can be determined for each type of vibration, see Table I. The mobility curves for symmetrical vibrations show also resonance at 18 and

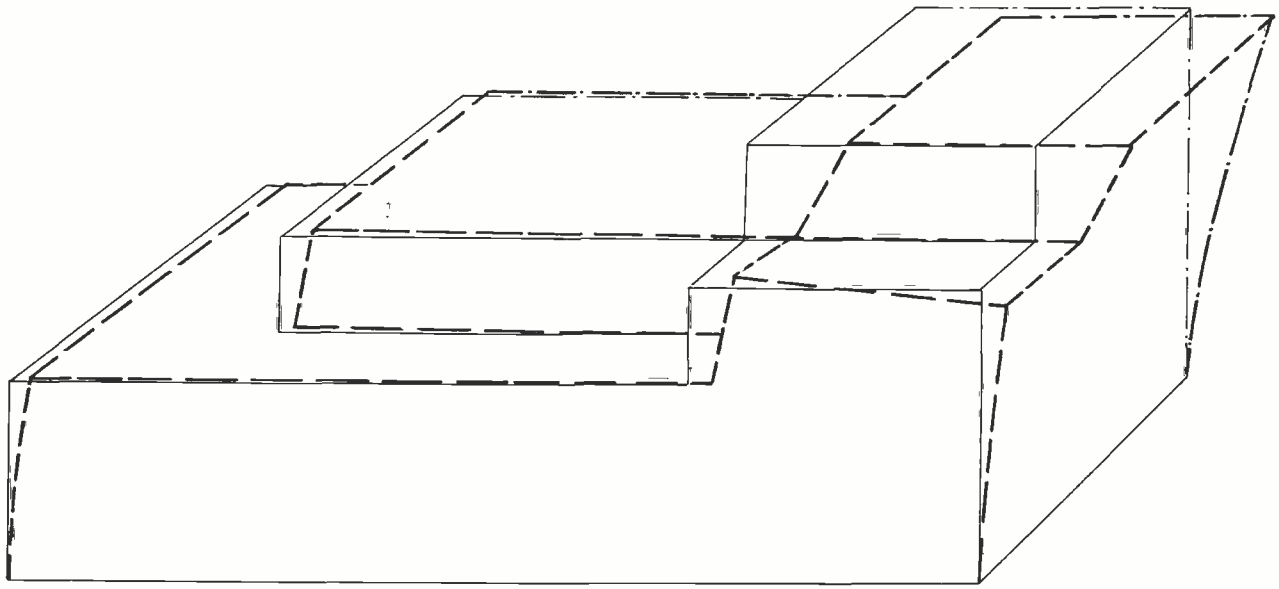

Fig. 8. 1st symmetric vibration mode (21.6 Hz), theoretical analysis.

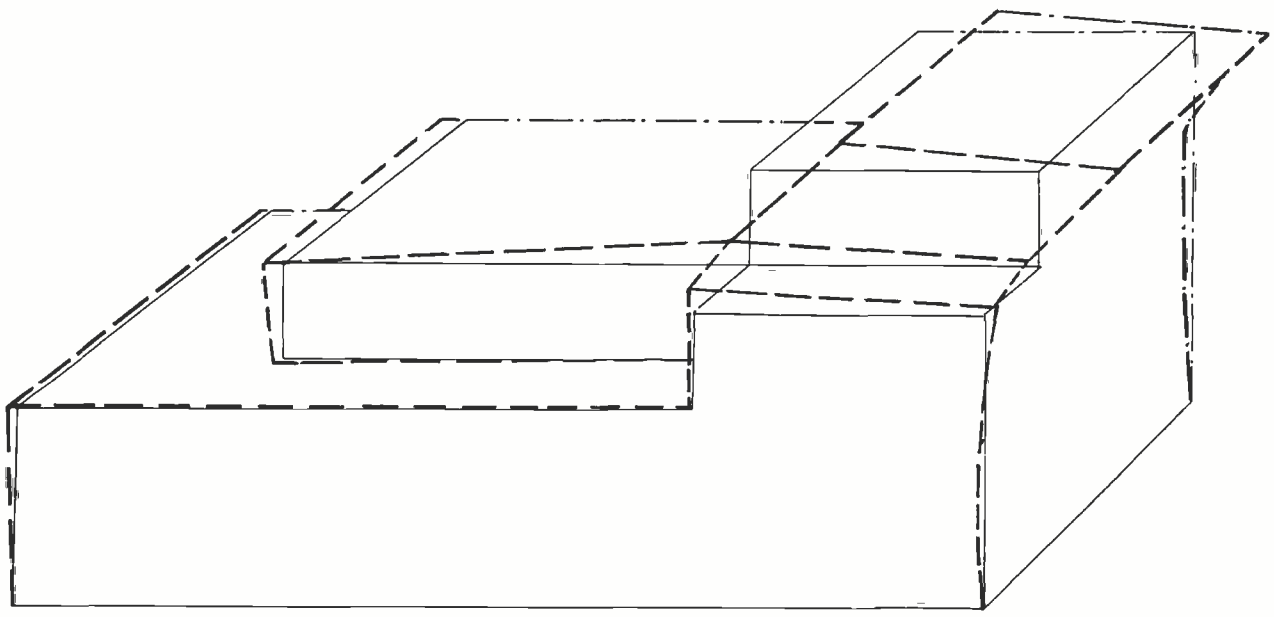

Fig. 9. 2nd symmetric vibration mode (27.8 Hz), theoretical analysis.

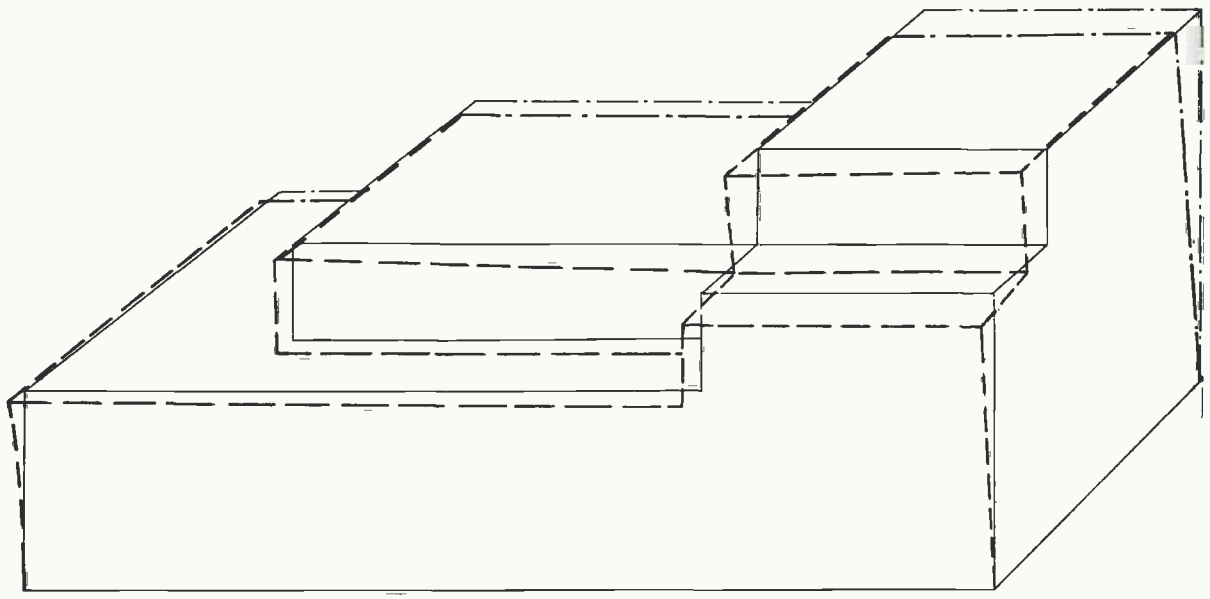

Fig. 10. 1st antisymmetric vibration mode (17.8 Hz), theoretical analysis.

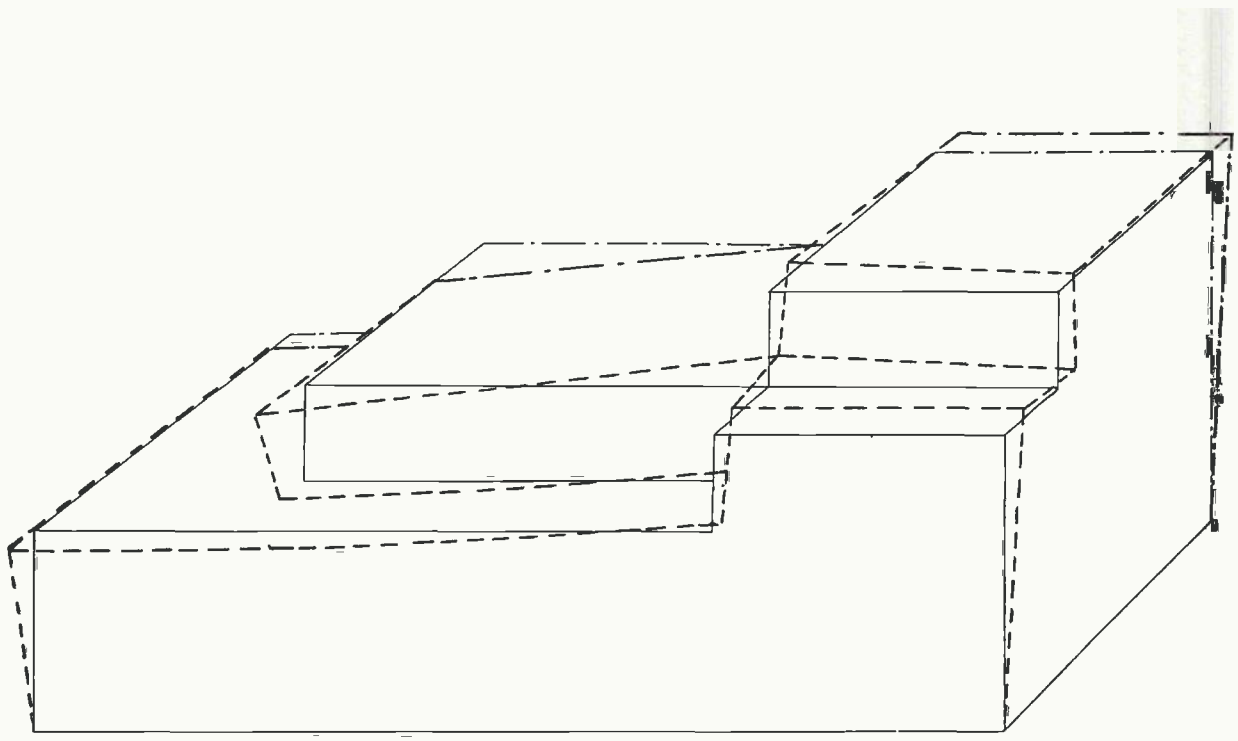

Fig. 11. 2nd antisymmetric vibration mode (26.7 Hz), theoretical analysis.

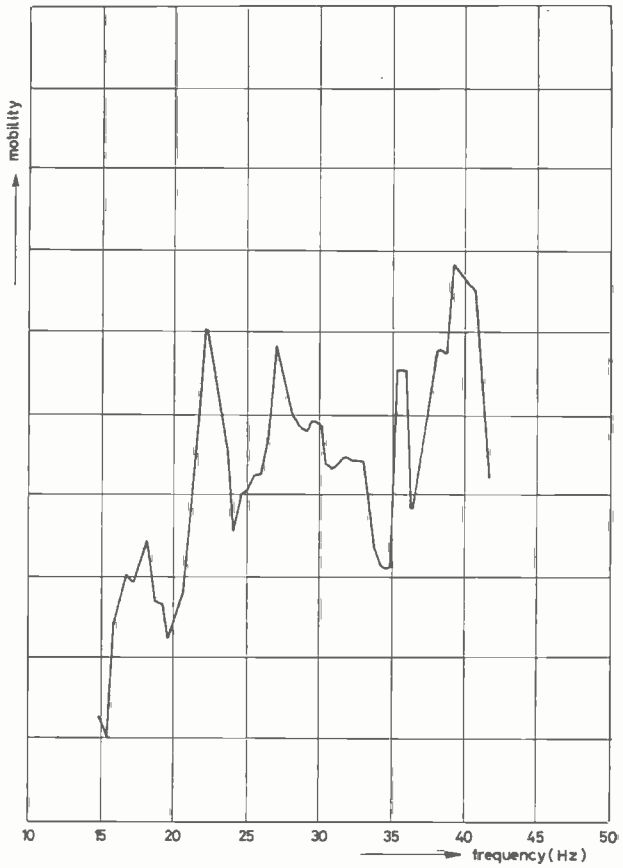

Fig. 12. Location 19: longitudinal excitation, longitudinal motion.

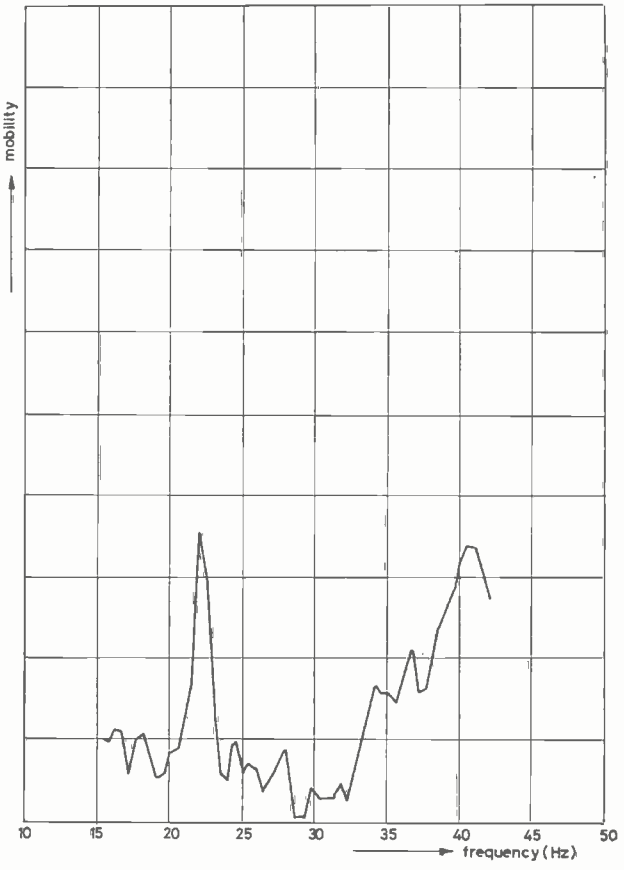

Fig. 13. Location 21: longitudinal excitation, longitudinal motion.

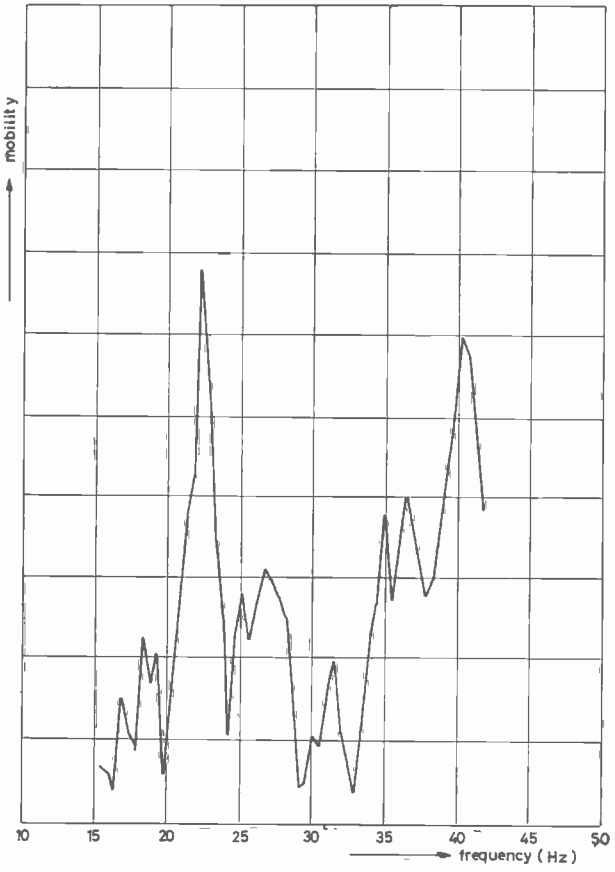

Fig. 14. Location 53: longitudinal excitation, longitudinal motion.

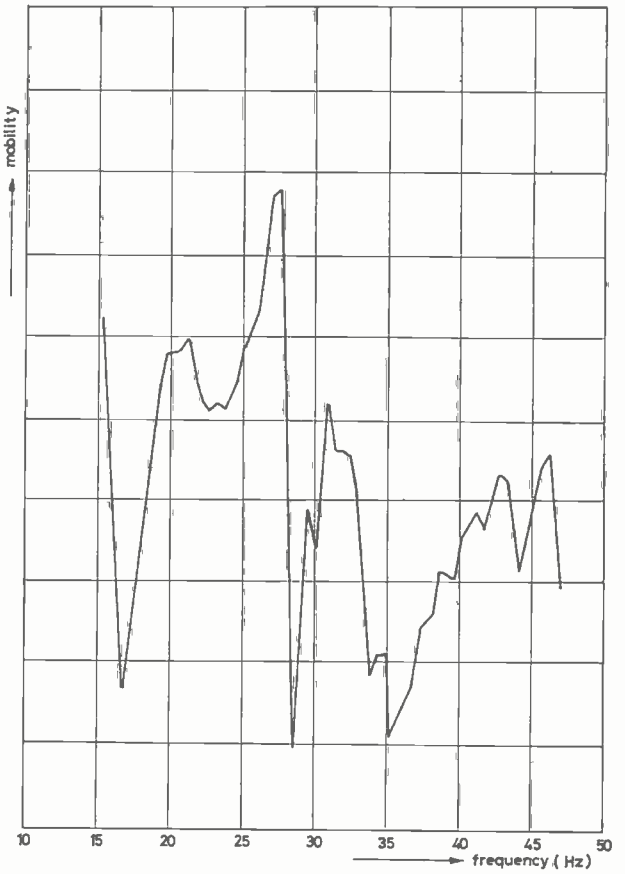

Fig. 15. Location 20: lateral excitation, lateral motion.

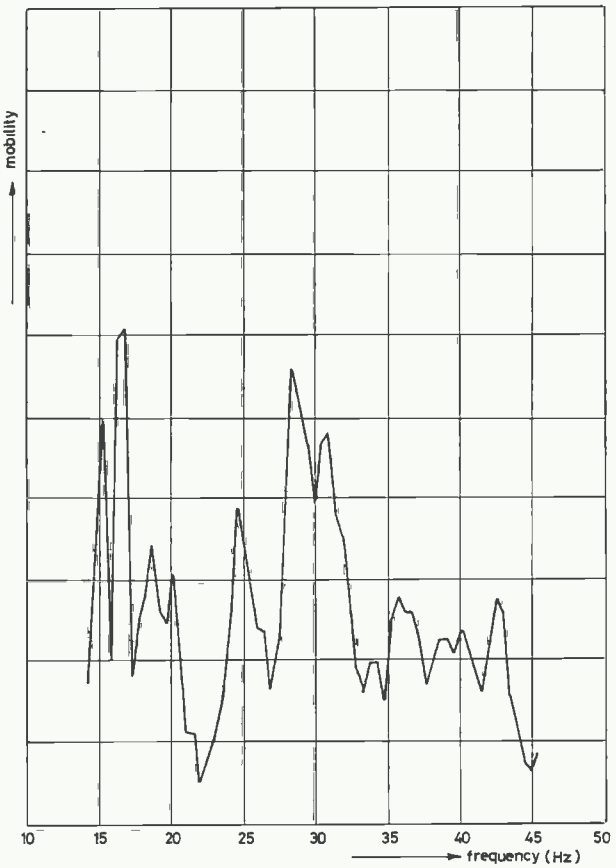

Fig. 16. Location 23: lateral excitation, lateral motion.

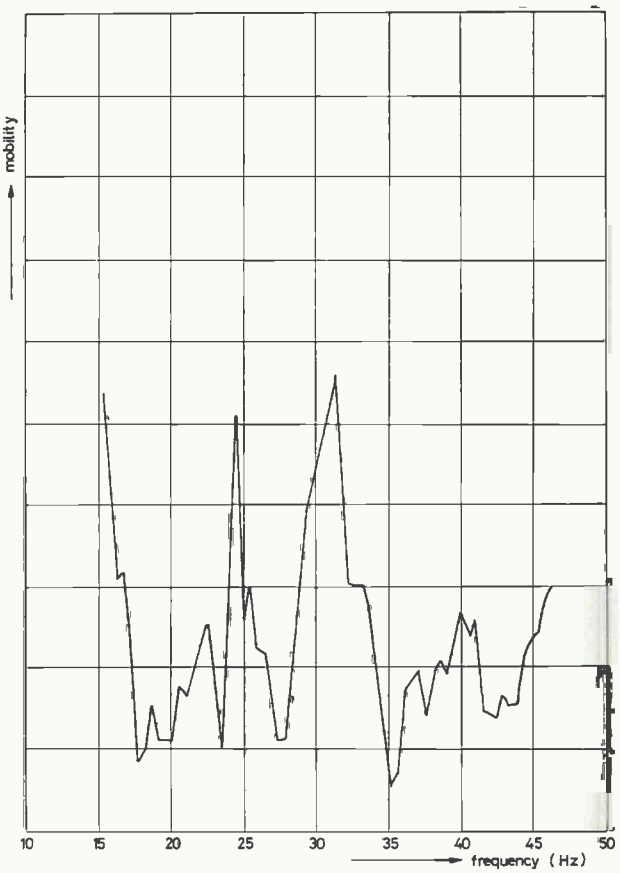

Fig. 17. Location 55: lateral excitation, lateral motion.

35 Hz, however, from a further examination of the displacement amplitudes at other points it was concluded that these were local plate field resonances which had not been incorporated in the theoretical analysis. The same holds for the resonance peaks at 20 and 42 Hz in case of antisymmetrical vibrations. The vibration modes corresponding to the theoretical vibration modes indicated in figs. 8–11 are shown in figs. 18–21.

The experimental and theoretical results for the lower resonance frequencies are in good agreement with each other. Taking into account all the approximations in modelling the structure for the theoretical analysis, the agreement is better than one would expect. The vertical displacements at the aftside of the deckhouse are considerable for symmetric vibrations and hence a rigid support as assumed in the analysis is a poor approximation but nevertheless the influence on the corresponding natural frequencies turns out to be small.

The lower resonance frequencies obtained with design stage data as discussed in section 4 are also presented in Table I; the total mass was in that case 566.8 t. The mass is about 6% more than the real mass and the influence of this difference on the lower natural frequencies will be that these frequencies are reduced by about 3%. The vibration modes of the two lower natural frequencies of each type as resulting from these calculations show only little local deviati s from the corresponding ones shown in figs. 8–11.

The procedure followed for the design stage solution implies that there may be strong, local deviations from the real mass and stiffness distribution but averaged over the structure these distributions are fairly accurate. A comparison of the approximate lower natural frequencies with the more accurate theoretical and the

Table I. Natural frequencies (Hz)

Symmetrical vibrations

mode	accurate analysis (total mass 531.7 t)	experiment	design stage analysis (566.8 t)
1	21.59	22	20.80
2	27.80	27	28.94
3	36.47	40	34.53
4	39.30	–	36.04
5	41.77	–	39.50

Antisymmetrical vibrations

mode	accurate analysis (total mass 531.7 t)	experiment	design stage analysis (566.8
1	17.76	16	17.99
2	26.69	25	25.68
3	30.14	31	29.93
4	34.04	–	31.18
5	39.13	–	34.92

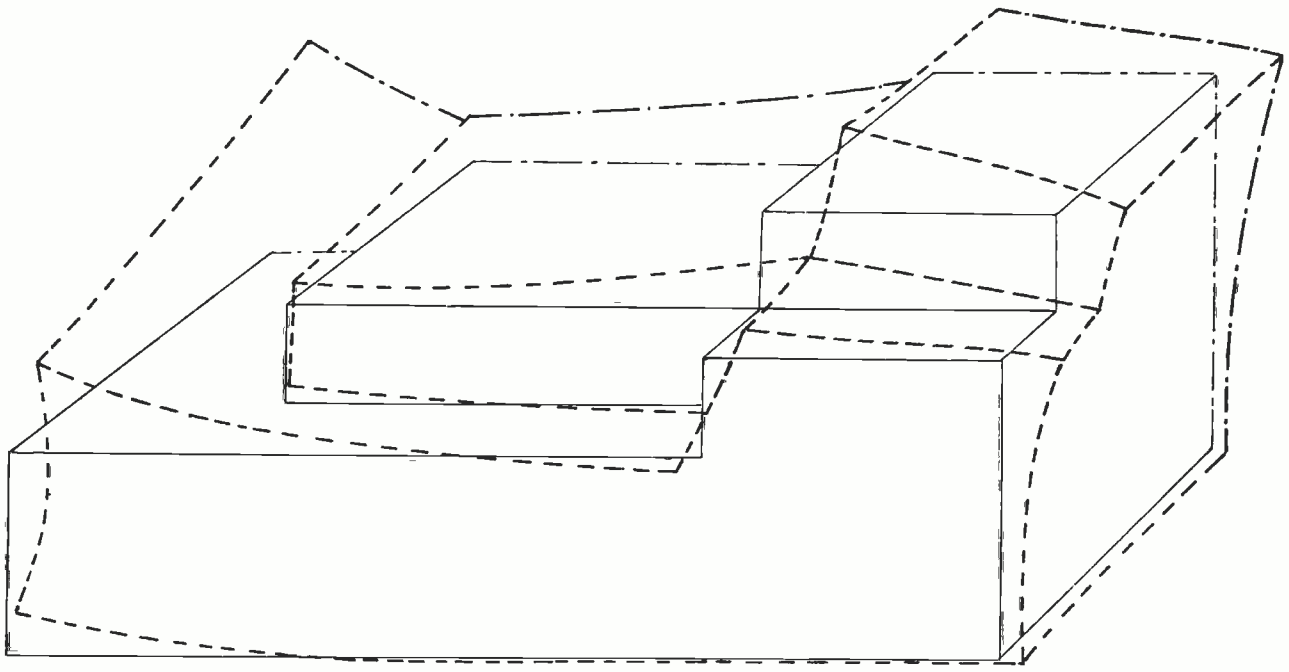

Fig. 18. 1st symmetric vibration mode (22 Hz), experimental analysis.

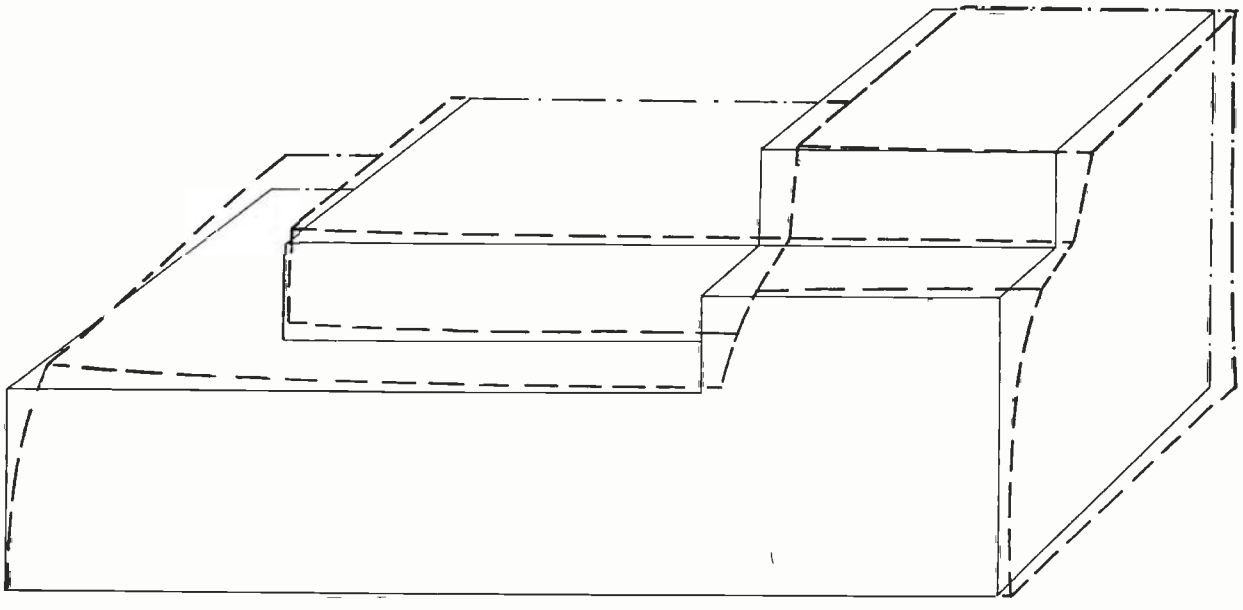

Fig. 19. 2nd symmetric vibration mode (27 Hz), experimental analysis.

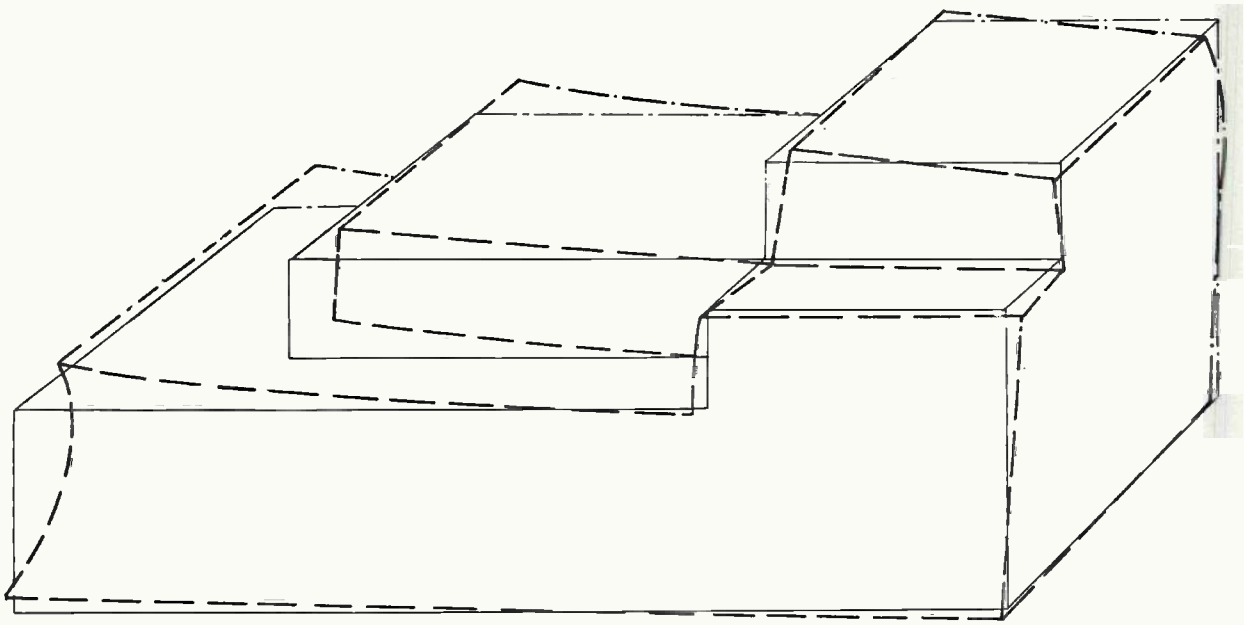

Fig. 20. 1st antisymmetric vibration mode (16 Hz), experimental analysis.

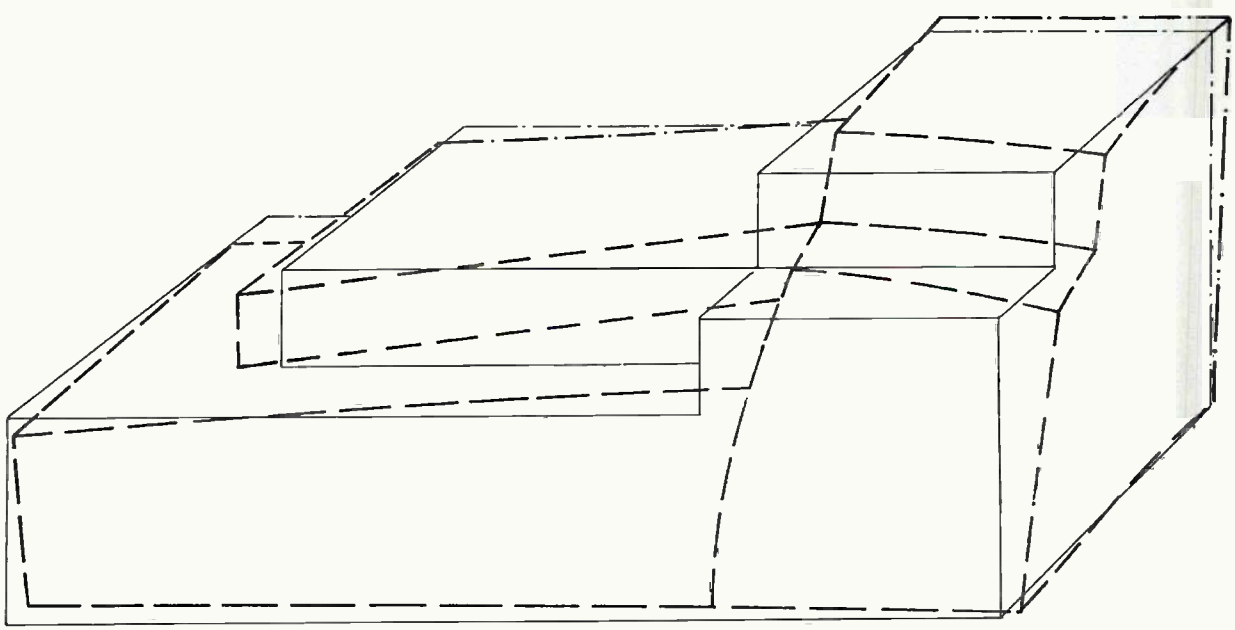

Fig. 21. 2nd antisymmetric vibration mode (25 Hz), experimental analysis.

experimental results in Table I shows that the accuracy of the approximate solution is remarkable.

The most rigorous theoretical solution of the problem would be obtained when the whole ship including the deckhouse and the influencing water around the ship is considered as a dynamic system for which the natural frequencies are to be determined. This gives at the same time the hull vibrations that have anyhow to be determined for a ship to be built. For certain vibration modes the deckhouse will behave as rigidly connected to the rest of the ship but there will also be modes that are practically local vibration modes of the deckhouse. Such an analysis is far more costly mainly in preparing the input data, than the method discussed in this report.

A first approximation to take into account the coupling of the deckhouse with the rest of the ship could be that the local stiffness coupling of the deckhouse with the undership is taken into account. Since the inplane stiffness of the main deck will be very high a restriction to the effect of the vertical flexibility will be sufficient as is also verified by the experimental results. For an existing ship this effect may be measured as indicated in Appendix III, whereas in the design stage a local finite element analysis can provide the required stiffness data.

6 Conclusions and remarks

a. The lowest natural frequency of the deckhouse has a sidewards vibration mode. The measured frequency is 16 Hz and the theoretically obtained frequency 17.8 Hz. It is to be expected that there is not a strong excitation of this vibration mode. The second frequency has a symmetrical mode and the motion is in longitudinal direction. The measured and calculated frequencies are 22 and 21.6 Hz respectively. The excitation forces near the screw will in general give stronger excitation of the symmetrical modes than the antisymmetrical modes and therefore it is necessary to look carefully at the excitation forces with a frequency of approximately 22 Hz.

   The third mode is an antisymmetrical one which shows mainly torsion of the deckhouse. The corresponding measured and calculated frequencies are 25 and 26.7 Hz.

b. Concluding from the design stage calculations it can be said that the values of the lower natural frequencies can be predicted rather accurately in an early stage of design.

c. It turns out that the effect of the coupling with the rest of the ship, although it affects the vibration mode, hardly influences the lower frequences. However, one must be very careful in generalizing such a statement with respect to other ships. Further research will be carried out in the nearest future with respect to this point for a tanker and a containership.

d. A second simplification introduced is that the deckhouse with many shifted bulkheads has been modelled to a regular box-structure and the effect of this modelling has been taken into account approximately by adapting the elastic constants of the plate elements. This introduces errors difficult to estimate and it still requires a considerable amount of work. These errors turn out to be small in the present case. When high values are wanted for the natural frequencies it is advisable to make a-simple regular structure. This will also qive more reliable results of the analysis.

e. Due to the availability of large finite element programmes with many different element types built in, such complicated structures can now be analysed in a rather short time without any computer programming. Only the modelling and description of the geometry have to be prepared.

f. In the analysis the local vibrations of plate panels or the local vibrations of equipment that is more or less flexibly supported, for example equipment in the funnel, are not incorporated. Such problems can easily be treated as local vibration problems, and the natural frequencies can be shifted by local stiffening.

References

1. K.N.S.M., Gewichten Bovenbouw „TRIDENT" Schepen.
2. Visser, W., The finite element method in deformation and heat conduction problems. Thesis, Delft 1968.
3. Cate, W. ten and P. Meijers, Berekening van eigenfrequenties en trillingsvormen van de bovenbouw van een schip. (Analysis of natural frequencies and vibration modes of the superstructure of a ship) TNO-IWECO 4671/1, April 1970.
4. Anderson, R. G., B. M. Irons and O. C. Zienkiewicz, Vibration and stability of plates using finite elements. Int. J. Solids Structures, 4, 1031–1055 (1968).
5. Zurmühl, R., Matrizen 2. Auflage Springer Verlag Berlin 1958.
6. Ramsden, J. N. and J. R. Stoker, Mass condensation: A semi-automatic method for reducing the size of vibration problems. Int. J. of Numerical Methods in Engineering, 1, 333–349 (1969).
7. Franz, A. K., Beproeving 5-tons excitator 35–100 Hz.
8. Wevers, L. J., Excitatiemeting van eigenfrequenties en trillingsvormen van de bovenbouw van het m.s. Trident, Rotterdam. TNO-IWECO 10096, augustus 1971.
9. Lloyds Register of Shipping Rep. SR 6417, March 1964. Distribution of leight weight for still water bending moment calculation of cargo ships.
10. Lloyds Register of Shipping Rep. The leight weight of a tanker.

APPENDIX I

Elastic constants for equivalent orthotropic plates

First the equations are to be derived for the elastic constants of the orthotropic field which replaces a plate field stiffened by regularly spaced stiffeners in x- and y-direction (Fig. 2).

The average normal stresses in the fictitious orthotropic plate are in terms of the plate and stiffener stresses:

$$\sigma_x = \sigma_{xp} + \frac{A_{xs}}{A_{pl}}\sigma_{xs}$$
$$\sigma_y = \sigma_{yp} + \frac{A_{ys}}{A_{pl}}\sigma_{ys} \qquad \text{(A-1)}$$

Since the strains in x- and y-direction are equal for the plate and the stiffeners, the following relations hold:

$$\sigma_{xs} = \sigma_{xp} - \nu\sigma_{yp}$$
$$\sigma_{ys} = -\nu\sigma_{xp} + \sigma_{yp} \qquad \text{(A-2)}$$

With equations (A-1) and (A-2) one can express the four stress components and hence also the strains in terms of the fictitious stresses σ_x and σ_y of the orthotropic plate. The effective elastic constants E_1, E_2, and $\nu_{12}E_2 = \nu_{21}E_1$ of the orthotropic plate are now defined by the following relations between the average stress and strain components in the equivalent plate:

$$\varepsilon_x = \frac{1}{E_1}\sigma_x - \frac{\nu_{21}}{E_2}\sigma_y$$
$$\varepsilon_y = -\frac{\nu_{12}}{E_1}\sigma_x + \frac{1}{E_2}\sigma_y \qquad \text{(A-3)}$$

It follows from (A-1)–(A-3) that for the general case $A_{xs} \neq 0$ and $A_{ys} \neq 0$:

$$\frac{E_1}{E} = \frac{1 + \left(\frac{A_{xs}+A_{ys}}{A_{pl}}\right) + (1-\nu^2)\frac{A_{xs}A_{ys}}{A_{pl}^2}}{1+(1-\nu^2)\frac{A_{ys}}{A_{pl}}} \qquad \text{(A-4a)}$$

$$\frac{E_2}{E} = \frac{1 + \left(\frac{A_{xs}+A_{ys}}{A_{pl}}\right) + (1-\nu^2)\frac{A_{xs}A_{ys}}{A_{pl}^2}}{1+(1-\nu^2)\frac{A_{xs}}{A_{pl}}} \qquad \text{(A-4b)}$$

$$\frac{\nu_{12}}{\nu} = \frac{E_1}{E_2}\frac{\nu_{21}}{\nu} = \frac{1}{1+(1-\nu^2)\frac{A_{ys}}{A_{pl}}} \qquad \text{(A-4c)}$$

It will be clear that for stiffeners parallel to the x- and y-axis, the effective shear modulus G_{12} is equal to the shearmodulus of the plate material G.

Several plate elements contain fairly large openings or local stiffening and in a number of cases the plate element does not fit exactly between the nodes. At certain places there are intermediate bulkheads the stiffness of which has to be incorporated in the nearest bulkheads of the simplified structure. In all these cases an approximate relation between the load and he displacements has been calculated from which fictitious elastic constants for the plate elements could be obtained.

This procedure has also been followed for shifted bulkheads. Due to the shift the vertical stiffness is strongly reduced because of bending deformation. This bending deformation is again approximated and incorporated in the elastic constants of the plates.

APPENDIX II

Contribution of heavy apparatus to mass matrix

To obtain the contribution of a number of heavy apparatus to the structural mass-matrix, these apparatus have been handled as rigid bodies connected to a number of nodal points in the structure. This will be illustrated with fig. 22. This figure shows an apparatus in the plane of symmetry of the structure. For symmetric vibrations the degrees of freedom are the displacement u^* and v^* of the centre of gravity, and the rotation ψ_z^*. The mass is assumed to be m and the moment of inertia around the z-axis I_z. The virtual work of the inertia forces is for virtual variations of the freedoms u^*, v^* and ψ_z^*

$$|\delta u^* \delta v^* \delta \psi_z^*| |\overline{M}| \begin{vmatrix} \ddot{u}^* \\ \ddot{v}^* \\ \ddot{\psi}_z^* \end{vmatrix} \tag{A-5}$$

where

$$\overline{M} = \begin{vmatrix} m & 0 & 0 \\ 0 & m & 0 \\ 0 & 0 & I_z \end{vmatrix} \tag{A-6}$$

The relation between the nodal point displacements and the degrees of freedom at the centre of gravity is approximately as follows:

$$\begin{vmatrix} u^* \\ v^* \\ \psi_z^* \end{vmatrix} = D^* \begin{vmatrix} u_1 \\ v_1 \\ u_2 \\ v_2 \end{vmatrix} \tag{A-7}$$

where

$$D^* = \begin{vmatrix} \frac{c_2}{(c_1+c_2)} & -\frac{a}{(c_1+c_2)} & \frac{c_1}{(c_1+c_2)} & \frac{a}{(c_1+c_2)} \\ 0 & \frac{c_2}{(c_1+c_2)} & 0 & \frac{c_1}{(c_1+c_2)} \\ 0 & \frac{a}{(c_1+c_2)} & 0 & -\frac{a}{(c_1+c_2)} \end{vmatrix} \tag{A-8}$$

Substitution of (A-7) into (A-5) yields the contribution of this apparatus to the mass matrix:

$$M_1 = D'^* \overline{M} D^* \tag{A-9}$$

With a location matrix this contribution can be placed in the structural mass matrix. In case of antisymmetrical vibrations and for all other apparatus a similar procedure may be followed.

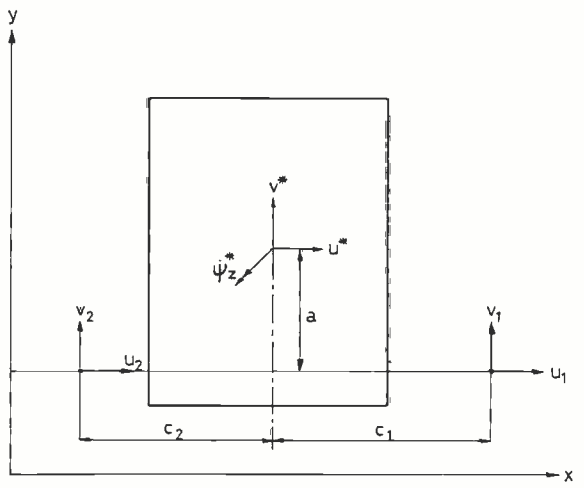

Fig. 22. Rigid body connected to nodal points 1 and 2

APPENDIX III

Determination of the stiffness-coupling from mobility measurements

It is assumed that for the simplified deckhouse shown in fig. 23 the velocity amplitudes and hence the displacement amplitudes at the basepoints (1–6) for a prescribed harmonic excitation are known from experiments.

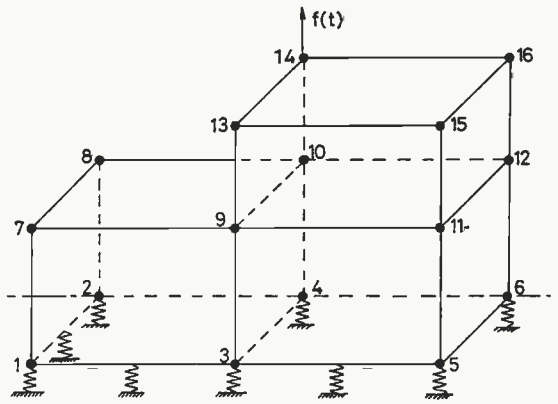

Fig. 23. Simplified deckhouse.

The vector of amplitudes of displacement-components coupled with the elastic support is defined to be v_1 and the remaining part of the vector of displacement amplitudes v is defined v_2.

The elastic energy in the deckhouse excluding the support can formally be written as:

$$E_d = \tfrac{1}{2} v' S v \qquad \text{(A-10)}$$

where S is the stiffness matrix which is assumed to be known from a finite element analysis. The elastic energy in the foundation is written in the form:

$$E_f = \tfrac{1}{2} v' C v \qquad \text{(A-11)}$$

where C is the matrix to be evaluated.

When M is the mass matrix (which is assumed to be available) and damping is neglected, the set of equations for the displacement amplitudes in terms of the amplitudes of the excitation force(s) is:

$$|S + C - \omega^2 M| v = f \qquad \text{(A-12)}$$

In case the structure is not excited at a point of the foundation which is a logical assumption, equation (A-12) may be rewritten in the form:

$$\begin{vmatrix} S_{11} & S_{12} \\ S_{21} & S_{22} \end{vmatrix} \begin{vmatrix} v_1 \\ v_2 \end{vmatrix} + \ldots$$

$$+ \begin{vmatrix} C_{11} & 0 \\ 0 & 0 \end{vmatrix} \begin{vmatrix} v_1 \\ v_2 \end{vmatrix} - \omega^2 \begin{vmatrix} M_{11} & M_{12} \\ M_{21} & M_{22} \end{vmatrix} \begin{vmatrix} v_1 \\ v_2 \end{vmatrix} = \begin{vmatrix} 0 \\ f_2 \end{vmatrix} \qquad \text{(A-13)}$$

Mostly f_2 has only one non-zero component. From (A-13) it follows for the displacement-components not in contact with the foundation:

$$v_2 = [S_{22} - \omega^2 M_{22}]^{-1} | f_2 - (S_{21} - \omega^2 M_{21}) v_1 | \qquad \text{(A-14)}$$

and

$$C_{11} v_1 = -|S_{11} - \omega^2 M_{11}| v_1 - |S_{12} - \omega^2 M_{12}| [S_{22} - \omega^2 M_{22}]^{-1} | f_2 - (S_{21} - \omega^2 M_{21}) v_1 | \qquad \text{(A-15)}$$

In case the stiffness of the foundation is discretized by a number of springs connected at the chosen nodal points, matrix C_{11} is a diagonal matrix. In that case the diagonal terms of C_{11} may in principle be obtained from an excitation at one point with one frequency, provided of course that none of the components of vector v_1 is equal to zero. The displacement amplitudes for points not coupled with the foundation follow from (A-14) when these displacements are also measured, the experiment and the analysis may be compared at this point. When the mass is discretized such that M is a diagonal mass matrix, equation (A-14) may be applied to determine the diagonal terms of M_{22}.

In the more general case that C_{11} is not a diagonal matrix this matrix may be obtained from the response on a sufficient number of vectors f_2 or frequencies ω. It will be clear that the analysis is valid only between the natural frequencies. In case the excitation frequency is a natural frequency of the system, the amplitudes are restricted only due to damping and this has not been taken into account in the analysis.

PUBLICATIONS OF THE NETHERLANDS SHIP RESEARCH CENTRE TNO

LIST OF EARLIER PUBLICATIONS AVAILABLE ON REQUEST
PRICE PER COPY DFL. 10.— (POSTAGE NOT INCLUDED)

M = engineering department S = shipbuilding department C = corrosion and antifouling department

Reports

90 S Computation of pitch and heave motions for arbitrary ship forms. W. E. Smith, 1967.
91 M Corrosion in exhaust driven turbochargers on marine diesel engines using heavy fuels. R. W. Stuart Mitchell, A. J. M. S. van Montfoort and V. A. Ogale, 1967.
92 M Residual fuel treatment on board ship. Part II. Comparative cylinder wear measurements on a laboratory diesel engine using filtered or centrifuged residual fuel. A de Mooy, M. Verwoest and G. G. van der Meulen, 1967.
93 C Cost relations of the treatments of ship hulls and the fuel consumption of ships. H. J. Lageveen-van Kuijk, 1967.
94 C Optimum conditions for blast cleaning of steel plate. J. Remmelts, 1967.
95 M Residual fuel treatment on board ship. Part I. The effect of centrifuging, filtering and homogenizing on the unsolubles in residual fuel. M. Verwoest and F. J. Colon, 1967.
96 S Analysis of the modified strip theory for the calculation of ship motions and wave bending moments. J. Gerritsma and W. Beukelman, 1967.
97 S On the efficacy of two different roll-damping tanks. J. Bootsma and J. J. van den Bosch, 1967.
98 S Equation of motion coefficients for a pitching and heaving destroyer model. W. E. Smith, 1967.
99 S The manoeuvrability of ships on a straight course. J. P. Hooft, 1967.
100 S Amidships forces and moments on a $C_B = 0.80$ "Series 60" model in waves from various directions. R. Wahab, 1967.
101 C Optimum conditions for blast cleaning of steel plate. Conclusion. J. Remmelts, 1967.
102 M The axial stiffness of marine diesel engine crankshafts. Part I. Comparison between the results of full scale measurements and those of calculations according to published formulae. N. J. Visser, 1967.
103 M The axial stiffness of marine diesel engine crankshafts. Part II. Theory and results of scale model measurements and comparison with published formulae. C. A. M. van der Linden, 1967.
104 M Marine diesel engine exhaust noise. Part I. A mathematical model. J. H. Janssen, 1967.
105 M Marine diesel engine exhaust noise. Part II. Scale models of exhaust systems. J. Buiten and J. H. Janssen, 1968.
106 M Marine diesel engine exhaust noise. Part III. Exhaust sound criteria for bridge wings. J. H. Janssen en J. Buiten, 1967.
107 S Ship vibration analysis by finite element technique. Part I. General review and application to simple structures, statically loaded. S. Hylarides, 1967.
108 M Marine refrigeration engineering. Part I. Testing of a decentralised refrigerating installation. J. A. Knobbout and R. W. J. Kouffeld, 1967.
109 S A comparative study on four different passive roll damping tanks. Part I. J. H. Vugts, 1968.
110 S Strain, stress and flexure of two corrugated and one plane bulkhead subjected to a lateral, distributed load. H. E. Jaeger and P. A. van Katwijk, 1968.
111 M Experimental evaluation of heat transfer in a dry-cargo ships' tank, using thermal oil as a heat transfer medium. D. J. van der Heeden, 1968.
112 S The hydrodynamic coefficients for swaying, heaving and rolling cylinders in a free surface. J. H. Vugts, 1968.
113 M Marine refrigeration engineering. Part II. Some results of testing a decentralised marine refrigerating unit with R 502. J. A. Knobbout and C. B. Colenbrander, 1968.
114 S The steering of a ship during the stopping manoeuvre. J. P. Hooft, 1969.
115 S Cylinder motions in beam waves. J. H. Vugts, 1968.
116 M Torsional-axial vibrations of a ship's propulsion system. Part I. Comparative investigation of calculated and measured torsional–axial vibrations in the shafting of a dry cargo motorship. C. A. M. van der Linden, H. H. 't Hart and E. R. Dolfin, 1968.
117 S A comparative study on four different passive roll damping tanks. Part II. J. H. Vugts, 1969.
118 M Stern gear arrangement and electric power generation in ships propelled by controllable pitch propellers. C. Kapsenberg, 1968.
119 M Marine diesel engine exhaust noise. Part IV. Transferdamping data of 40 modelvariants of a compound resonator silencer. J. Buiten, M. J. A. M. de Regt and W. P. Hanen, 1968.
120 C Durability tests with prefabrication primers in use steel of plates. A. M. van Londen and W. Mulder, 1970.
121 S Proposal for the testing of weld metal from the viewpoint of brittle fracture initiation. W. P. van den Blink and J. J. W. Nibbering, 1968.
122 M The corrosion behaviour of cunifer 10 alloys in seawaterpiping-systems on board ship. Part I. W. J. J. Goetzee and F. J. Kievits, 1968.
123 M Marine refrigeration engineering. Part III. Proposal for a specification of a marine refrigerating unit and test procedures. J. A. Knobbout and R. W. J. Kouffeld, 1968.
124 S The design of U-tanks for roll damping of ships. J. D. van den Bunt, 1969.
125 S A proposal on noise criteria for sea-going ships. J. Buiten, 1969.
126 S A proposal for standardized measurements and annoyance rating of simultaneous noise and vibration in ships. J. H. Janssen, 1969.
127 S The braking of large vessels II. H. E. Jaeger in collaboration with M. Jourdain, 1969.
128 M Guide for the calculation of heating capacity and heating coils for double bottom fuel oil tanks in dry cargo ships. D. J. van der Heeden, 1969.
129 M Residual fuel treatment on board ship. Part III. A. de Mooy, P. J. Brandenburg and G. G. van der Meulen, 1969.
130 M Marine diesel engine exhaust noise. Part V. Investigation of a double resonatorsilencer. J. Buiten, 1969.
131 S Model and full scale motions of a twin-hull vessel. M. F. van Sluijs, 1969.
132 M Torsional-axial vibrations of a ship's propulsion system. Part II. W. van Gent and S. Hylarides, 1969.
133 S A model study on the noise reduction effect of damping layers aboard ships. F. H. van Tol, 1970.
134 M The corrosion behaviour of cunifer-10 alloys in seawaterpiping-systems on board ship. Part II. P. J. Berg and R. G. de Lange, 1969.
135 S Boundary layer control on a ship's rudder. J. H. G. Verhagen, 1970.
136 S Observations on waves and ship's behaviour made on board of Dutch ships. M. F. van Sluijs and J. J. Stijnman, 1971.
137 M Torsional-axial vibrations of a ship's propulsion system. Part III. C. A. M. van der Linden, 1969.
138 S The manoeuvrability of ships at low speed. J. P. Hooft and M. W. C. Oosterveld, 1970.
139 S Prevention of noise and vibration annoyance aboard a sea-going passenger and carferry equipped with diesel engines. Part I. Line of thoughts and predictions. J. Buiten, J. H. Janssen, H. F. Steenhoek and L. A. S. Hageman, 1971.
140 S Prevention of noise and vibration annoyance aboard a sea-going passenger and carferry equipped with diesel engines. Part II. Measures applied and comparison of computed values with measurements. J. Buiten, 1971.
141 S Resistance and propulsion of a high-speed single-screw cargo liner design. J. J. Muntjewerf, 1970.
142 S Optimal meteorological ship routeing. C. de Wit, 1970.
143 S Hull vibrations of the cargo-liner "Koudekerk". H. H. 't Hart, 1970.
144 S Critical consideration of present hull vibration analysis. S. Hylarides, 1970.
145 S Computation of the hydrodynamic coefficients of oscillating cylinders. B. de Jong, 1973.
146 M Marine refrigeration engineering. Part IV. A Comparative study on single and two stage compression. A. H. van der Tak, 1970.
147 M Fire detection in machinery spaces. P. J. Brandenburg, 1971.
148 S A reduced method for the calculation of the shear stiffness of a ship hull. W. van Horssen, 1971.
149 M Maritime transportation of containerized cargo. Part II. Experimental investigation concerning the carriage of green coffee from Colombia to Europe in sealed containers. J. A. Knobbout, 1971.
150 S The hydrodynamic forces and ship motions in oblique waves. J. H. Vugts, 1971.

151 M Maritime transportation of containerized cargo. Part I. Theoretical and experimental evaluation of the condensation risk when transporting containers loaded with tins in cardboard boxes. J. A. Knobbout, 1971.
152 S Acoustical investigations of asphaltic floating floors applied on a steel deck. J. Buiten, 1971.
153 S Ship vibration analysis by finite element technique. Part II. Vibration analysis. S. Hylarides, 1971.
155 M Marine diesel engine exhaust noise. Part VI. Model experiments on the influence of the shape of funnel and superstructure on the radiated exhaust sound. J. Buiten and M. J. A. M. de Regt, 1971.
156 S The behaviour of a five-column floating drilling unit in waves. J. P. Hooft, 1971.
157 S Computer programs for the design and analysis of general cargo ships. J. Holtrop, 1971.
158 S Prediction of ship manoeuvrability. G. van Leeuwen and J. M. J. Journée, 1972.
159 S DASH computer program for Dynamic Analysis of Ship Hulls. S. Hylarides, 1971.
160 M Marine refrigeration engineering. Part VII. Predicting the control properties of water valves in marine refrigerating installations A. H. van der Tak, 1971.
161 S Full-scale measurements of stresses in the bulkcarrier m.v. 'Ossendrecht'. 1st Progress Report: General introduction and information. Verification of the gaussian law for stress-response to waves. F. X. P. Soejadi, 1971.
162 S Motions and mooring forces of twin-hulled ship configurations. M. F. van Sluijs, 1971.
163 S Performance and propeller load fluctuations of a ship in waves. M. F. van Sluijs, 1972.
164 S The efficiency of rope sheaves. F. L. Noordegraaf and C. Spaans, 1972.
165 S Stress-analysis of a plane bulkhead subjected to a lateral load. P. Meijers, 1972.
166 M Contrarotating propeller propulsion, Part I, Stern gear, line shaft system and engine room arrangement for driving contrarotating propellers. A. de Vos, 1972.
167 M Contrarotating propeller propulsion. Part II. Theory of the dynamic behaviour of a line shaft system for driving contrarotating propellers. A. W. van Beek, 1972.
169 S Analysis of the resistance increase in waves of a fast cargo ship. J. Gerritsma and W. Beukelman, 1972.
170 S Simulation of the steering- and manoeuvring characteristics of a second generation container ship. G. M. A. Brummer, C. B. van de Voorde, W. R. van Wijk and C. C. Glansdorp, 1972.
172 M Reliability analysis of piston rings of slow speed two-stroke marine diesel engines from field data. P. J. Brandenburg, 1972.
173 S Wave load measurements on a model of a large container ship. Tan Seng Gie, 1972.
174 M Guide for the calculation of heating capacity and heating coils for deep tanks. D. J. van der Heeden and A. D. Koppenol, 1972.
176 S Bow flare induced springing. F. F. van Gunsteren, 1973.
177 M Maritime transportation of containerized cargo. Part III. Fire tests in closed containers. H. J. Souer, 1973.
178 S Fracture mechanics and fracture control for ships. J. J. W. Nibbering, 1973.
179 S Effect of forward draught variation on performance of full ships. M. F. van Sluijs and C. Flokstra, 1973.
184 S Numerical and experimental vibration analysis of a deckhouse. P. Meijers, W. ten Cate, L. J. Wevers and J. H. Vink, 1973.

Communications

15 M Refrigerated containerized transport (Dutch). J. A. Knobbout, 1967.
16 S Measures to prevent sound and vibration annoyance aboard a seagoing passenger and carferry, fitted out with dieselengines (Dutch). J. Buiten, J. H. Janssen, H. F. Steenhoek and L. A. S. Hageman, 1968.
17 S Guide for the specification, testing and inspection of glass reinforced polyester structures in shipbuilding (Dutch). G. Hamm, 1968.
18 S An experimental simulator for the manoeuvring of surface ships. J. B. van den Brug and W. A. Wagenaar, 1969.
19 S The computer programmes system and the NALS language for numerical control for shipbuilding. H. le Grand, 1969.
20 S A case study on networkplanning in shipbuilding (Dutch). J. S. Folkers, H. J. de Ruiter, A. W. Ruys, 1970.
21 S The effect of a contracted time-scale on the learning ability for manoeuvring of large ships (Dutch). C. L. Truijens, W. A. Wagenaar, W. R. van Wijk, 1970.
22 M An improved stern gear arrangement. C. Kapsenberg, 1970.
23 M Marine refrigeration engineering. Part V (Dutch). A. H. van der Tak, 1970.
24 M Marine refrigeration engineering. Part VI (Dutch). P. J. G. Goris and A. H. van der Tak, 1970.
25 S A second case study on the application of networks for productionplanning in shipbuilding (Dutch). H. J. de Ruiter, H. Aartsen, W. G. Stapper and W. F. V. Vrisou van Eck, 1971.
26 S On optimum propellers with a duct of finite length. Part II. C. A. Slijper and J. A. Sparenberg, 1971.
27 S Finite element and experimental stress analysis of models of shipdecks, provided with large openings (Dutch). A. W. van Beek and J. Stapel, 1972.
28 S Auxiliary equipment as a compensation for the effect of course instability on the performance of helmsmen. W. A. Wagenaar, P. J. Paymans, G. M. A. Brummer, W. R. van Wijk and C. C. Glansdorp, 1972.
29 S The equilibrium drift and rudder angles of a hopper dredger with a single suction pipe. C. B. van de Voorde, 1972.
30 S A third case study on the application of networks for productionplanning in shipbuilding (Dutch). H. J. de Ruiter and C. F. Heijnen, 1973.
31 S Some experiments on one-side welding with various backing materials. Part I. Manual metal arc welding with coated electrodes and semi-automatic gas shielded arc welding (Dutch). J. M. Vink, 1973.
32 S The application of computers aboard ships. Review of the state of the art and possible future developments (Dutch). G. J. Hogewind and R. Wahab, 1973.
33 S FRODO, a computerprogram for resource allocation in networkplanning (Dutch). H. E. I. Bodewes, 1973.
34 S Bridge design on dutch merchant vessels; an ergonomic study. Part I: A summary of ergonomic points of view (Dutch). A. Lazet, H. Schuffel, J. Moraal, H. J. Leebeek and H. van Dam, 1973.
35 S Bridge design on dutch merchant vessels; an ergonomic study. Part II: First results of a questionnaire completed by captains, navigating officers and pilots. J. Moraal, H. Schuffel and A. Lazet, 1973.
36 S Bridge design on dutch merchant vessels; an ergonomic study. Part III: Observations and preliminary recommendations. A. Lazet, H. Schuffel, J. Moraal, H. J. Leebeek and H. van Dam, 1973.

DECK - E.

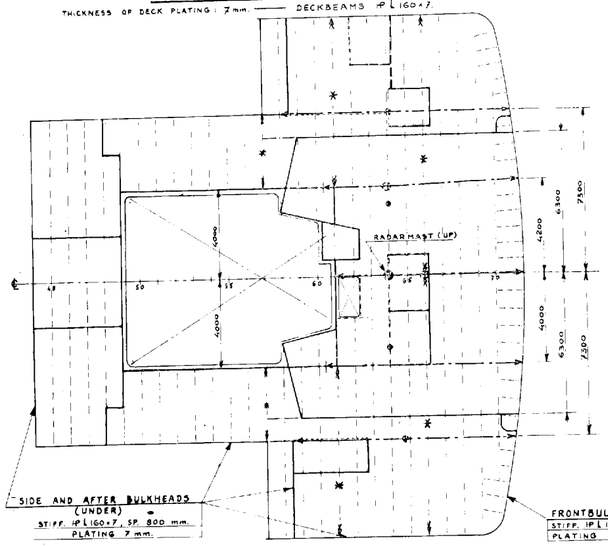

DECK - F.

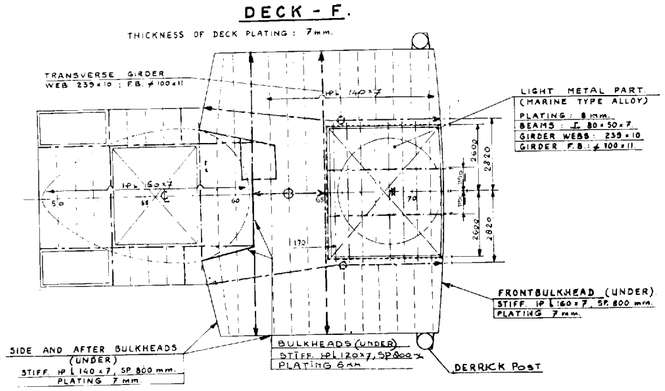

FRAME - 53. (PORT) FRAME - 68 (STARBOARD)

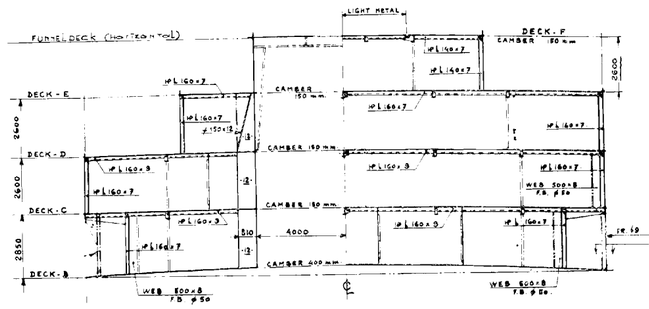

FRAME - 54 (STARBOARD)

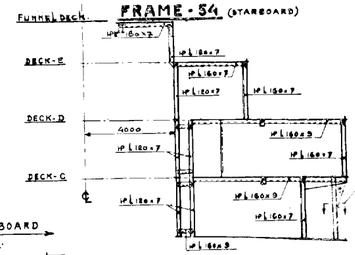

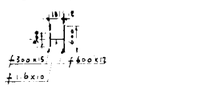

DECK - D.

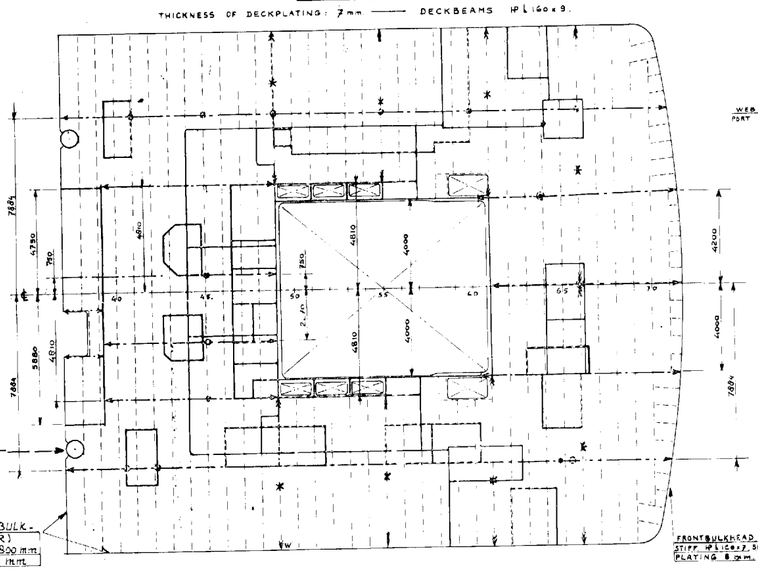

LONGITUDINAL SECTION AT ℄.

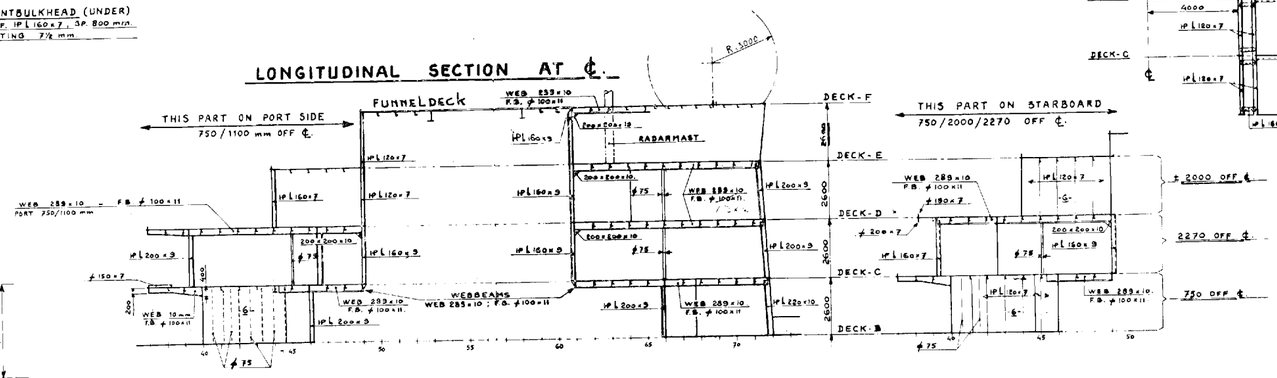

LONGITUDINAL SECTION 4000/4810 mm OFF ℄. (PORT SIDE)

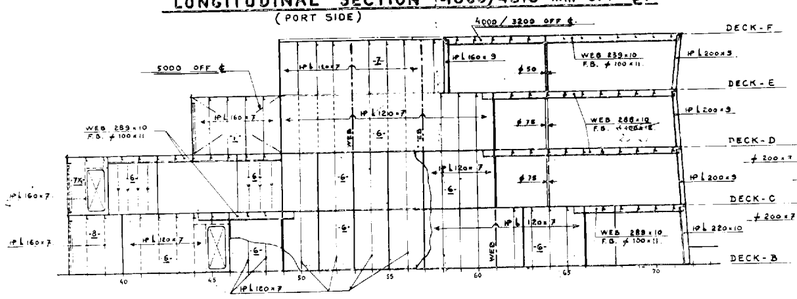

LONGITUDINAL SECTION 4000/4810 mm OFF ℄. (STARBOARD SIDE)

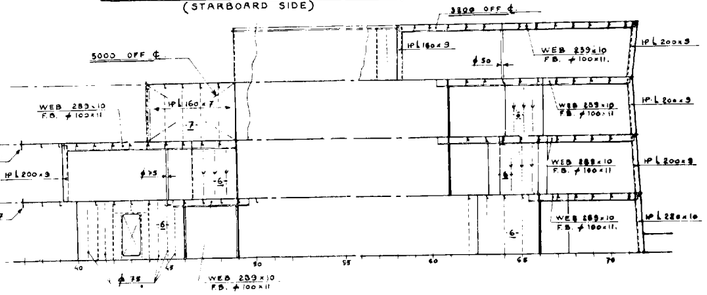

DECK - C.

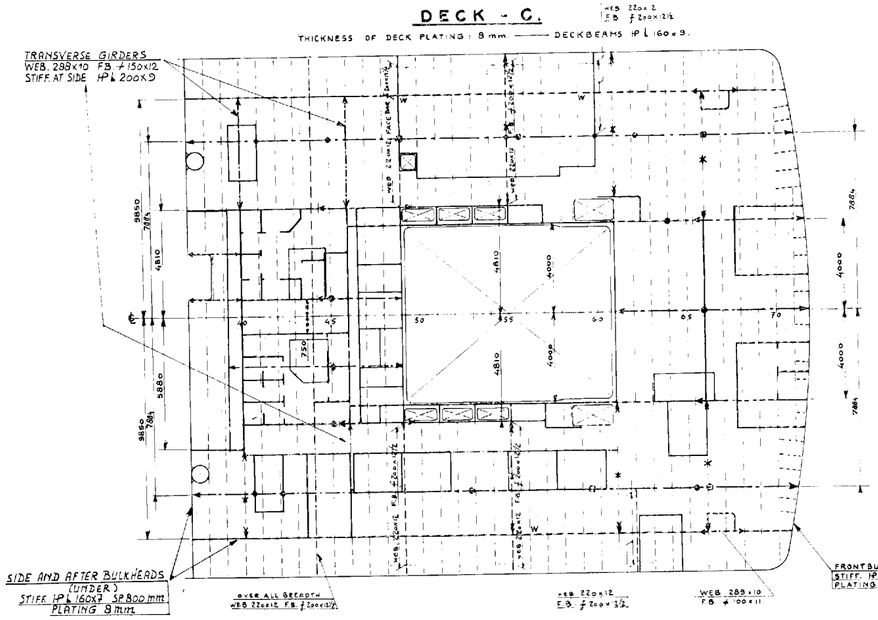

LONGITUDINAL SECTION 7300/7884 mm OFF ℄. (PORT SIDE)

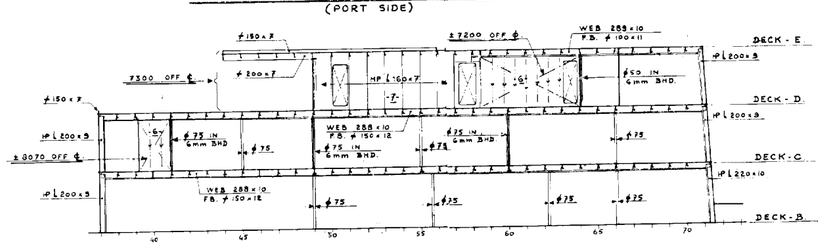

LONGITUDINAL SECTION 7300/7884 mm OFF ℄. (STARBOARD SIDE)

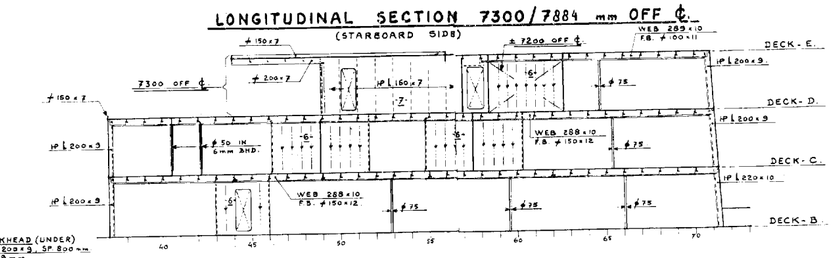

Construction Plan
Bridge Deckhouse

REMARKS :

● = PILLAR UP.
○ = PILLAR UNDER.
W = WEB AT SIDE UNDER.
✱ = REINFORCED BEAM HP L 220 x 10.
FRAME SPACING 800 mm.